

Level 3 Tsunami Modelling in Hawke's Bay Final Report

DR Burbidge
B Lukovic

JH Roger
WL Power

X Wang

**GNS Science Consultancy Report 2022/58
June 2022**



DISCLAIMER

This report has been prepared by the Institute of Geological and Nuclear Sciences Limited (GNS Science) exclusively for and under contract to Hawke's Bay Regional Council. GNS Science accepts no responsibility for any use of or reliance on any contents of this report by any person other than Hawke's Bay Regional Council and shall not be liable to any person other than Hawke's Bay Regional Council, on any ground, for any loss, damage or expense arising from such use or reliance. However, in the event that, notwithstanding this statement of disclaimer, GNS Science is at law held to have a duty of care to a third party, liability to that third party shall be excluded and limited under the contract with Hawke's Bay Regional Council. Any party using or relying on this report will be regarded as having accepted the terms of this disclaimer.

Use of Data:

Date that GNS Science can use associated data: July 2022

BIBLIOGRAPHIC REFERENCE

Burbidge DR, Roger JH, Wang X, Lukovic B, Power WL. 2022. Level 3 tsunami modelling in Hawke's Bay final report. Lower Hutt (NZ): GNS Science. 52 p. Consultancy Report 2022/58.

CONTENTS

EXECUTIVE SUMMARY	IV
1.0 INTRODUCTION	1
1.1 Project Design	3
1.1.1 Stage 1: Scenario Selection	3
1.1.2 Stage 2: Digital Elevation Model Creation.....	3
1.1.3 Stage 3: Tsunami Inundation Modelling	4
1.1.4 Stage 4: Hazard Maps.....	4
2.0 SCENARIO SELECTION	5
2.1 Deaggregating the National Tsunami Hazard Model.....	5
2.2 Determining the Earthquake Source Parameters.....	10
3.0 DIGITAL ELEVATION MODEL CREATION	15
3.1 Global Digital Elevation Model	15
3.2 New Zealand Digital Elevation Model	15
3.3 Hawke’s Bay Digital Elevation Model.....	15
4.0 TSUNAMI INUNDATION MODELLING	18
4.1 Simulation Software: COMCOT	18
4.2 Reference Level and Terminologies	18
4.3 Modelling Grid Set-Up	19
4.4 Roughness Model.....	22
4.5 Special Treatment with Low-Lying Dry Land.....	23
4.6 Effects of Earth Curvature, Rotation and High Latitude.....	24
4.7 Other Simulation Settings	25
4.8 Test Runs	25
4.9 Final Models	26
5.0 PROBABILISTIC TSUNAMI INUNDATION HAZARD MAPS	28
6.0 DISCUSSION	47
7.0 ACKNOWLEDGEMENTS	49
8.0 REFERENCES	49

FIGURES

Figure 1.1	Tsunami coastal zones offshore the Hawke’s Bay region	2
Figure 1.2	The area of interest for the project	4
Figure 2.1	Tsunami hazard curves for Zone 73 in NHTM2021 and NTHM2013.....	5
Figure 2.2	Maps showing the location of the faults for each of the scenarios listed in Tables 2.1 and 2.2	8
Figure 3.1	Details of the nearshore bathymetry of the digital elevation model	16
Figure 3.2	The high-resolution (~5 m) DEM created to model the inundation in Zones 73 and part of Zone 74	17
Figure 4.1	Illustration of some definitions used in tsunami modelling	19

Figure 4.2	Coverage of modelling grid 01 for the Hawke's Bay modelling.....	20
Figure 4.3	Coverage of modelling grid 02.....	21
Figure 4.4	Coverage of modelling grid 04, which has the highest level of detail (~11 m) used for the modelling of tsunami inundation in the Hawke's Bay region.....	21
Figure 4.5	Spatial distribution of equivalent surface roughness values, i.e. Manning's n, in Hawke's Bay (grid 04) for tsunami inundation modelling.	23
Figure 4.6	Yellow polygons outline low-lying land areas around Hawke's Bay Airport and south of Ahuriri River Estuary	24
Figure 4.7	Example of the results of one of the test scenarios	26
Figure 4.8	Example of the inundation produced from a M_w 8.9 event on the Hikurangi subduction zone at MHWS for a return period of 2500 years	27
Figure 5.1	The DEM used grid 04 zoomed into Napier Harbour, Ahuriri Estuary and Ngaruroro Estuary ...	30
Figure 5.2	Probabilistic tsunami inundation maps for Hawke's Bay showing the median flow depths onshore and offshore tsunami heights with a 1-in-100-years chance of being exceeded per annum at current MHWS.....	31
Figure 5.3	Probabilistic tsunami inundation maps for Hawke's Bay showing the median flow depths onshore and offshore tsunami heights with a 1-in-100-years chance of being exceeded per annum at current MHWS plus 0.65 m of sea-level rise	32
Figure 5.4	Probabilistic tsunami inundation maps for Hawke's Bay showing the median flow depths onshore and offshore tsunami heights with a 1-in-100-years chance of being exceeded per annum at current MHWS plus 1 m of sea-level rise	33
Figure 5.5	Probabilistic tsunami inundation maps for Hawke's Bay showing the median flow depths onshore and offshore tsunami heights with a 1-in-100-years chance of being exceeded per annum at current MHWS plus 1.99 m of sea-level rise	34
Figure 5.6	Probabilistic tsunami inundation maps for Hawke's Bay showing the median flow depths onshore and offshore tsunami heights with a 1-in-500-years chance of being exceeded per annum at current MHWS.....	35
Figure 5.7	Probabilistic tsunami inundation maps for Hawke's Bay showing the median flow depths onshore and offshore tsunami heights with a 1-in-500-years chance of being exceeded per annum at current MHWS plus 0.65 m of sea-level rise	36
Figure 5.8	Probabilistic tsunami inundation maps for Hawke's Bay showing the median flow depths onshore and offshore tsunami heights with a 1-in-500-years chance of being exceeded per annum at current MHWS plus 1 m of sea-level rise	37
Figure 5.9	Probabilistic tsunami inundation maps for Hawke's Bay showing the median flow depths onshore and offshore tsunami heights with a 1-in-500-years chance of being exceeded per annum at current MHWS plus 1.99 m of sea-level rise	38
Figure 5.10	Probabilistic tsunami inundation maps for Hawke's Bay showing the median flow depths onshore and offshore tsunami heights with a 1-in-1000-years chance of being exceeded per annum at current MHWS.....	39
Figure 5.11	Probabilistic tsunami inundation maps for Hawke's Bay showing the median flow depths onshore and offshore tsunami heights with a 1-in-1000-years chance of being exceeded per annum at current MHWS of sea-level rise plus 0.65 m	40
Figure 5.12	Probabilistic tsunami inundation maps for Hawke's Bay showing the median flow depths onshore and offshore tsunami heights with a 1-in-1000-years chance of being exceeded per annum at current MHWS plus 1 m of sea-level rise	41
Figure 5.13	Probabilistic tsunami inundation maps for Hawke's Bay showing the median flow depths onshore and offshore tsunami heights with a 1-in-1000-years chance of being exceeded per annum at current MHWS plus 1.99 m of sea-level rise	42

Figure 5.14	Probabilistic tsunami inundation maps for Hawke’s Bay showing the 84 th percentile flow depths onshore and offshore tsunami heights with a 1-in-2500-years chance of being exceeded per annum at current MHWS.....	43
Figure 5.15	Probabilistic tsunami inundation maps for Hawke’s Bay showing the 84 th percentile flow depths onshore and offshore tsunami heights with a 1-in-2500-years chance of being exceeded per annum at current MHWS plus 0.65 m	44
Figure 5.16	Probabilistic tsunami inundation maps for Hawke’s Bay showing the 84 th percentile flow depths onshore and offshore tsunami heights with a 1-in-2500-years chance of being exceeded per annum at current MHWS plus 1 m	45
Figure 5.17	Probabilistic tsunami inundation maps for Hawke’s Bay showing the 84 th percentile flow depths onshore and offshore tsunami heights with a 1-in-2500-years chance of being exceeded per annum at current MHWS plus 1.99 m	46

TABLES

Table 2.1	The top six scenarios and their effective magnitudes for Zone 73 (Napier) determined by deaggregating NTHM2021 (Power et al. 2022) at four return periods: 100, 500, 1000 and 2500 years.....	6
Table 2.2	The top six scenarios and their effective magnitudes for Zone 74 (Cape Kidnappers) determined by deaggregating NTHM2021 (Power et al. 2022) at four return periods: 100, 500, 1000 and 2500 years.....	7
Table 2.3	The 31 scenarios, their effective magnitudes and the return periods used in this study.....	9
Table 2.4	Deaggregated source scenarios and the re-scaled slip and magnitude amount used in the inundation modelling for the 100-year return period hazard maps for Zone 73	10
Table 2.5	Deaggregated source scenarios and the re-scaled slip and magnitude amount used in the inundation modelling for the 500-year return period hazard maps for Zone 73	11
Table 2.6	Deaggregated source scenarios and the rescaled slip and magnitude amount used in the inundation modelling for the 1000-year return period hazard maps for Zone 73	11
Table 2.7	Deaggregated source scenarios and the rescaled slip and magnitude amount used in the inundation modelling for the 2500-year return period hazard map for Zone 73	12
Table 2.8	Deaggregated source scenarios and the re-scaled slip and magnitude amount used in the inundation modelling for the 100-year return period hazard maps for Zone 74	12
Table 2.9	Deaggregated source scenarios and the re-scaled slip and magnitude amount used in the inundation modelling for the 500-year return period hazard maps for Zone 74	13
Table 2.10	Deaggregated source scenarios and the re-scaled slip and magnitude amount used in the inundation modelling for the 1000-year return period hazard maps for Zone 74	13
Table 2.11	Deaggregated source scenarios and the re-scaled slip and magnitude amount used in the inundation modelling for the 2500-year return period hazard maps for Zone 74	14
Table 4.1	Nested grid set-up for tsunami simulations.....	22
Table 5.1	Scenario normalised contribution for Zone 73.....	28
Table 5.2	Scenario normalised contribution for Zones 74.....	29

EXECUTIVE SUMMARY

In November 2021, Hawke's Bay Regional Council (HBRC) commissioned GNS Science to provide them with tsunami hazard maps for Napier and surrounding areas that are appropriate for them to use for land-use planning in the region. To create maps suitable for this purpose, HBRC has requested that GNS Science conduct a study to create probabilistic tsunami inundation hazard maps to a Level 3 standard for the Napier/Hastings Coastal Hazard Zone. This is Zone 73 in the National Tsunami Hazard Model (NTHM; see Power et al. 2022). HBRC also requested that the area to be mapped is extended beyond the zone out to the neighbouring Cape Kidnappers Hazard Zone (Zone 74 in the NTHM) if that was appropriate. Maps were to cover four return periods: 100, 500, 1000 and 2500 years, and the latter return period needed to be consistent with the 'Maximum Considered Tsunami' as defined in the Ministry of Business, Innovation & Employment (MBIE) guidelines. Hazard maps were also required for four different sea-level heights: the present-day level at Mean High Water Springs (MHWS) and the MHWS level plus 0.65 m, 1.0 m and 1.99 m of sea-level rise. In total, 16 different hazard maps were requested for the area of interest for each coastal zone.

To produce these maps, GNS Science used the latest update to the NTHM (Power et al. 2022) to select scenarios appropriate for each return period for both Zone 73 and 74. The NTHM estimates the offshore tsunami height at a range of return periods, including those needed in this project. For all of the return periods investigated here, an earthquake on the Hikurangi Subduction Zone was the largest contributor to the tsunami hazard for both coastal zones. At the 100-year return period, the majority of the tsunami hazard for this return period comes from a Hikurangi earthquake with an effective moment magnitude (M_w) 8.3 megathrust earthquake. At the 2500-year return period, the majority of the hazard comes from an effective M_w 9.0 megathrust earthquake on the Hikurangi interface. Earthquake magnitudes in the NTHM are 'effective', rather than the actual seismic magnitude, as they also include a component to capture the effect of non-uniform slip on the resulting tsunami (see Power 2013 and Power et al. 2022).

However, the Hikurangi interface is not the only source of tsunami hazard for this area at these return periods. For the 100-year return period, most of the rest of the hazard to both coastal zones comes from regional and distant subduction zone earthquakes on subduction zones such as Peru, Chile, Kermadec and the Kuriles. At the 500-year return period, most of the rest of the hazard comes from a combination of earthquakes on local crust faults lying offshore New Zealand (such as the Lachlan Fault), the outer-rise faults and earthquakes on the Kermadec or Peru Subduction Zone interfaces. At the 2500-year return period, the top six sources of the hazard are all local sources, mostly from earthquakes on the Hikurangi interface but with a significant additional contribution from earthquakes on local crustal faults and local outer-rise faults as well.

GNS Science then combined LiDAR provided by HBRC with their existing bathymetry and topography to produce a Digital Elevation Model suitable for tsunami inundation modelling for the area of interest. Also, a grid of roughness values has been built in agreement with the actual land-cover data for Napier. This grid, and the scenarios described above, were then used to simulate the inundation expected from these scenarios in the region at each of the required sea levels. These were then combined using a weighted median approach to create probabilistic tsunami inundation maps for each return period and sea-level height combination. As expected, at the 100-year return period (i.e. the map showing the flow depths with a 1-in-100 chance of being exceeded each year, aka the 1:100-year map) the extent of inundation is small at the current MHWS, restrained to the low-lying area around Hawke's Bay Airport and the immediate

neighbourhood of rivers. However, at the 1000- and 2500-year return periods, the inundation extents are much larger, with most of the inundation occurring in Napier's coastal suburbs of Ahuriri and Awatoto, the low-lying area around the Hawke's Bay Airport, Napier Port and small towns south of the Tutaekuri river (i.e. Clive, Haumoana and Te Awanga). The effect of adding 0.65 m, 1 m or 1.99 m of sea-level rise projections is to increase the area inundated. The increase in area is substantial once 1.99 m is added to the current MHWS. This has the effect of increasing the frequency of a given area of inundation. For example, adding 1.99 m of sea-level rise to the model increases the area inundated by the 1:100-year tsunami (Figure 5.4) beyond that inundated by the 1:2500 event at the current MHWS (Figure 5.13). Increasing the sea level by these large amounts has a greater impact on the area inundated than increasing the return period within the ranges considered in this study.

This page left intentionally blank.

1.0 INTRODUCTION

Hawke's Bay Regional Council (HBRC) commissioned GNS Science to provide them with tsunami models for Hawke's Bay that are appropriate to use for land-use planning in the region. HBRC anticipates that, during preparation of the Kotahi Plan, a risk management approach to assessing hazard risks is likely to be taken and the risk then managed according to accepted thresholds. The available tsunami computer modelling completed to date for the area is deterministic (i.e. based on particular scenarios) and has not taken the probabilistic method now recommended for land-use planning. The National Emergency Management Agency (NEMA; formerly MCDEM) Director's Guidelines for Tsunami Evacuation Zones recommends the use of 'Level 3 or 4' probabilistic mapping to provide results with sufficient accuracy for land-use planning purposes. Level 3 modelling "uses a physics-based computer simulation of the process by which water inundates across land" from a tsunami to estimate the evacuation zones (MCDEM 2016). 'Level 4' modelling for evacuation zone design "is the most comprehensive approach, based on drawing an envelope around all inundations from many well-tested hydrodynamic computer models run from source through to inundation". These types of tsunami hazard map have been previously completed by GNS Science for Porirua, Wellington and Hutt City Councils primarily for land-use planning (Gusman et al. 2019a; Burbidge et al. 2021a; 2021b) and for Environment Canterbury for evacuation zone design (Mueller et al. 2019, 2020).

To create maps suitable for land-use planning, HBRC has requested that GNS Science conduct a study to create probabilistic tsunami hazard mapping to a Level 3 standard for the Napier/Hastings coastal zone (Zone 73 in Power [2013] and Power et al. [2022]). This zone is labelled as 'Napier' in Figure 1.1. HBRC also requested that the area to be modelled be extended beyond the zone out to Point 1 (location shown in Figure 1.1) in the Cape Kidnappers Zone (Zone 74), if that was feasible. Maps were to cover four return periods: 100, 500, 1000 and 2500 years, and the latter needed to be consistent with the 'Maximum Considered Tsunami' as defined in NEMA's Director's Guidelines for Tsunami Evacuation Zones (MCDEM 2016). The last set of maps are thus also suitable for informing the design of evacuation zones, primarily the Yellow Zone. On the other hand, the first set of maps for the 100-, 500- and 1000-year return periods are primarily designed for use in land-use planning.

Hazard maps were also required for four different sea-level heights: the present-day level at Mean High Water Springs (MHWS; which is 0.92 m above mean sea level [MSL] in this study for this area) and the MHWS level plus the 0.65 m, 1.0 m and 1.99 m of sea-level rise as requested by HBRC. This resulted in a total of 16 different hazard maps covering each coastal zone in the area of interest. The maps were required to show both the extents and depths of inundation (i.e. flow depths) at these return periods and sea-level assumptions. The maps were to be accompanied by a methodology report (this document). The methodology GNS Science has decided to use for this project is based on the ones used in previous similar studies completed for Porirua City Council (Gusman et al. 2019a) and then further developed in Burbidge et al. (2021a, 2021b) for Wellington and Hutt City Councils.

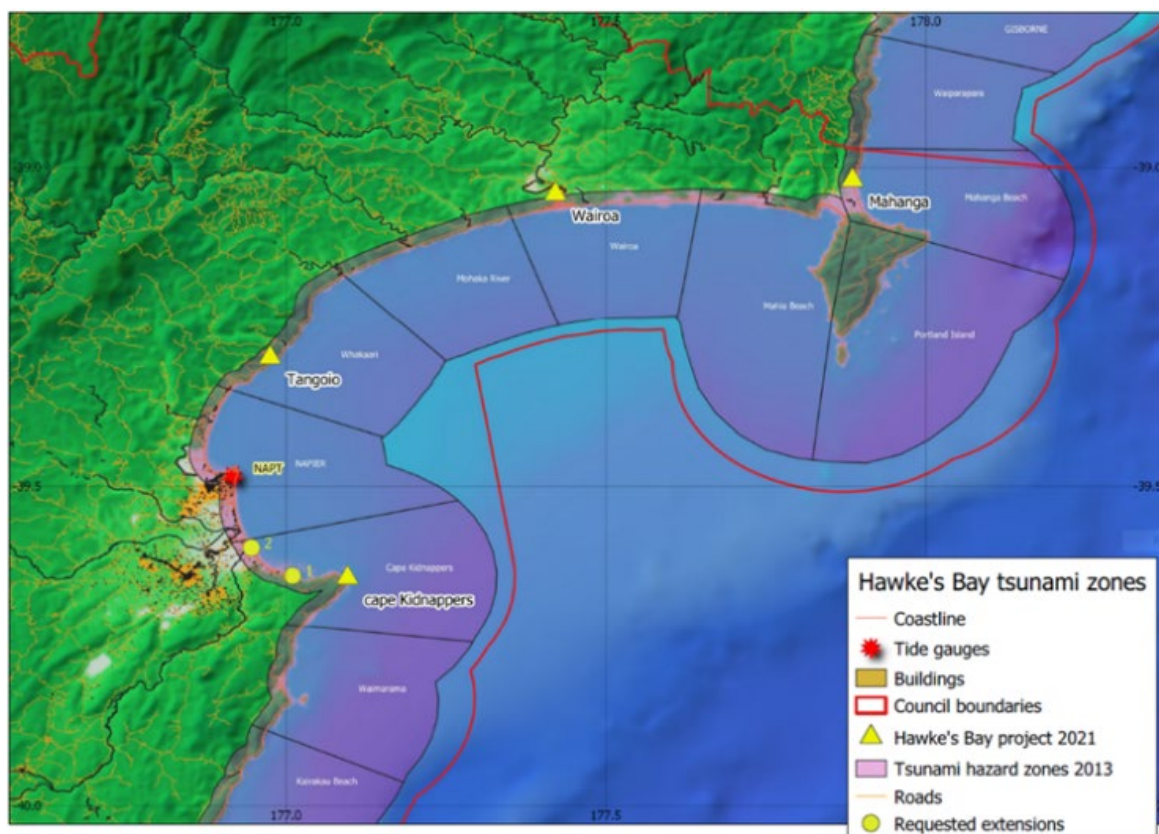


Figure 1.1 Tsunami coastal zones offshore the Hawke's Bay region. This project is limited to the area of LiDAR data provided by HBRC within the 'Napier' Hazard Zone extending out to Point '1', which is within the neighbouring Cape Kidnappers Tsunami Hazard Zone. The yellow triangles indicate the initial area of the study and thus the long-term requirements of HBRC.

The Earthquake Commission (EQC) are funding part of the cost of this project, and they require that the project also:

1. Demonstrate alignment with the three-year tsunami loss modelling project that EQC have commissioned GNS Science to complete.
2. Provide a pilot for the National Tsunami Hazard (or Risk) Model (NTHRM). The proposed NTHRM will provide New Zealand with a national, consistent tsunami hazard and risk model that is suitable for purposes such as land-use planning. This project will test the feasibility of this on a smaller spatial scale than is planned for the NTHRM and will produce a limited set of probabilistic tsunami inundation maps only (i.e. just the hazard, not the risk). Lessons learned from this study will be used to inform GNS Science on the issues and complexities of producing probabilistic tsunami inundation maps for a single coastal zone. This will then be used to inform GNS Science on what will need to be done to complete the much larger-scale NTHRM at a later date, if that project is funded.

1.1 Project Design

The project was structured into the following stages.

1.1.1 Stage 1: Scenario Selection

For each return period, the hazard in the Napier Zone (Zone 73) in the new NTHM model (NTHM2021; Power et al. 2022) was deaggregated, and six scenarios were selected for each return period that encompass the range of tsunamigenic earthquake sources that contribute to the hazard at that return period for the Napier Zone. For the 100-, 500- and 1000-year return periods, the median (50th percentile) hazard value for the zone was selected as the target, while the 84th percentile was used for the 2500-year period map. The 2500-year period map uses the 84th percentile (i.e. confidence level) rather than the 50th percentile to ensure that it meets the Ministry of Business, Innovation & Employment (MBIE) guidelines for the 'Maximum Considered Tsunami' as requested by HBRC (MCDEM 2016).

Since HBRC would like to extend the maps out beyond the Napier Zone (to Point 1 in Figure 1.1), we also need to determine whether any additional scenarios are required. To determine what the additional scenarios might be, we also deaggregated the hazard in the nearby Cape Kidnappers zone (Zone 74, see Figure 2.1) in the NTHM2021 to determine whether there are any scenarios in that deaggregation that are significantly different from those in the Napier zone. For the purposes of this study, an event is significantly different if it comes from a different source (i.e. fault) or from the same source but differs by more than 0.1 magnitude units or differs in location by more than a fault length. These additional scenarios were then included in the inundation modelling stage below. The results from the deaggregation of the NTHM2021 for Zones 73 and 74 are provided in Section 2.

1.1.2 Stage 2: Digital Elevation Model Creation

For the purpose of the tsunami inundation modelling, GNS Science created a 5 m resolution Digital Elevation Model (DEM) of the Napier region by combining existing topographic and bathymetric data. This DEM extent is shown on Figure 1.2 (red rectangle). Bathymetric data came from the extraction of nautical chart information and/or GNS Science's existing bathymetric survey datasets (see Section 3). Topographic data came from GNS Science's existing topographic datasets, as well as the LiDAR dataset provided by HBRC (pink polygon on Figure 1.2). GNS Science then integrated this topographic and bathymetry data into a single 5 m elevation grid and then down sampled it to about 11 m to produce a final grid to be used in the modelling stage. An 11 m grid was used to keep the computations tractable within the time available to complete this project. This grid was then tested to ensure modelling stability and to ensure that features such as stop banks were properly incorporated. Note that this grid has been designed solely for the purposes of producing tsunami models for the area and may not be suitable for other purposes (e.g. navigation). The resulting grid is provided as one of the deliverables and described further in Section 3.

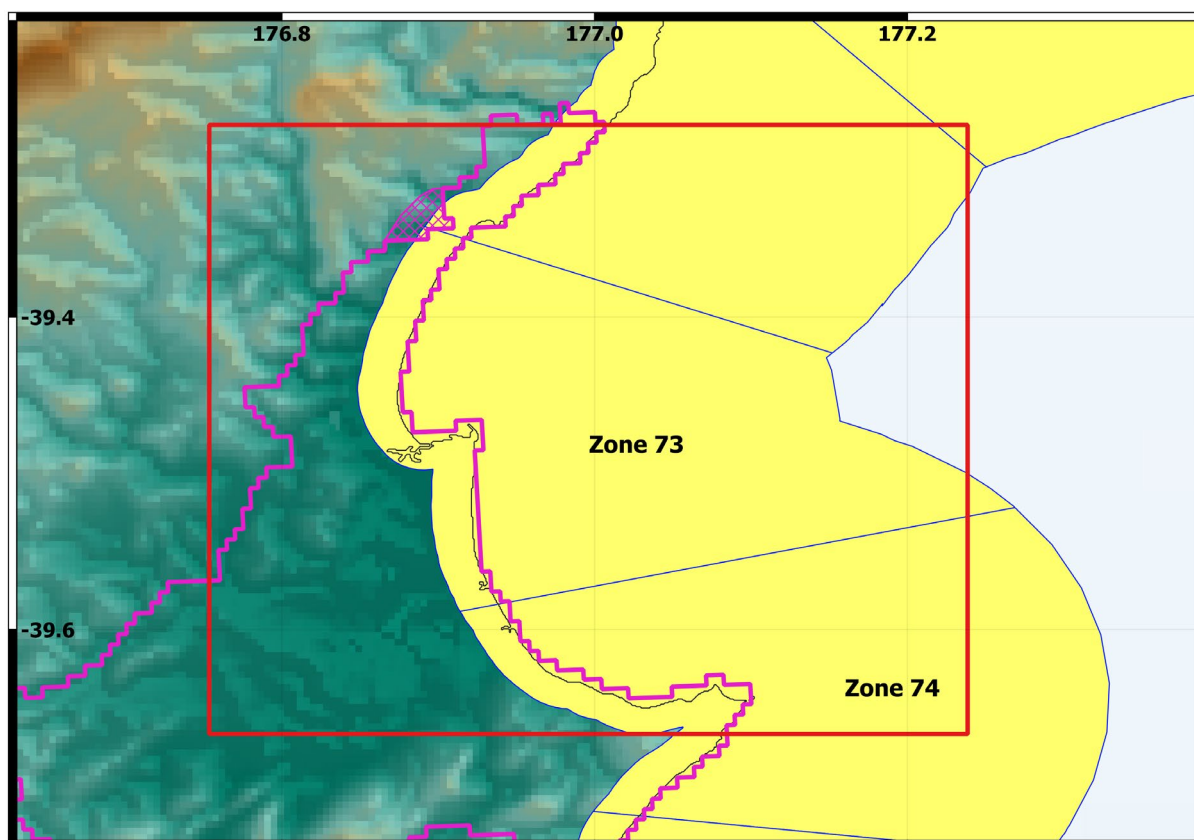


Figure 1.2 The area of interest for the project (red rectangle). HBRC's high-resolution LiDAR is shown by the pink polygon. The hatched pink polygon represents the zone where GNS Science asked HBRC for more LiDAR data. The current tsunami evacuation Yellow Zone is represented by the yellow-filled polygon.

1.1.3 Stage 3: Tsunami Inundation Modelling

After testing the stability of the new grids, each of the scenarios identified in Stage 1 were then modelled through to inundation in the area of interest. To do this, the models were run on either the High-Performance Computing Facility (HPCF) hosted within New Zealand's eScience Infrastructure (NeSI) or on GNS Science's own HPC system. At the end of this stage, we then had a set of scenarios with both the inundation extent and flow depths for each of them. These were run four times at each required sea-level value. In total, 134 tsunami models were completed through to inundation for the area of interest, all described further in Section 4.

1.1.4 Stage 4: Hazard Maps

Finally, from the set of scenarios calculated in Stage 3, GNS Science then created a series of tsunami hazard maps showing the median or 84th percentile inundation extent and flow depths region at each of the return periods and sea-level rise values specified. One set of maps were created for the scenarios used for Zone 73 and another for the scenarios appropriate for Zone 74. Since four return periods are required for four different sea-level rise values, a total of 32 maps are provided (16 for each coastal zone). Note also that the maps at the first three return periods (100, 500 and 1000 years) have been produced primarily to inform land-use planning in each coastal zone rather than to replace the existing evacuation zones maps. The maps have been provided to HBRC along with this report. The hazard map creation is described further in Section 5.

2.0 SCENARIO SELECTION

2.1 Deaggregating the National Tsunami Hazard Model

As stated earlier, we have based the scenarios for inundation modelling on the latest version of the NTHM2021. This new model has a variety of improvements; the main one relevant for this project being improved modelling of the tsunami from local sources. To achieve this improvement in the treating of local sources, we modelled tsunami caused by 248 local faults from around New Zealand based on estimates of fault geometry and plausible magnitudes of the earthquakes that could occur on each fault (Stirling et al. 2012; Power 2013). We also updated data and methods used in calculating tsunami heights from local-, regional- and distant-source subduction zones. This is further detailed in Power et al. (2022).

Figure 2.1a shows the updated hazard curves for Zone 73 (Napier) in the NTHM2021. For comparison, the hazard curves from the 2013 version of the NTHM (NTHM2013; Power 2013) are also shown (Figure 2.1b). The solid black line is the median hazard (as defined by the maximum offshore amplitude, i.e. tsunami height) as a function of the return period, while dashed lines show the 16% and 84% confidence intervals. The 16% and 84% confidence curves give an indication of the level of uncertainty in the hazard values for a given return period. Statistically, there is a 16% chance that the hazard will be below the lower dotted line and an 84% chance that it will be below the higher dotted line (and thus a 16% chance that it will be above it).

In the case shown here, the revised hazard estimated for Tsunami Hazard Zone 73 has gone up slightly. This appears to be mostly due to a larger contribution to the estimated hazard from outer-rise faults in the Hawke's Bay region, which more than compensates for a reduced contribution from South American distant sources, both of which are modelled using more accurate methods in the revised NTHM2021 than in the earlier NTHM2013.

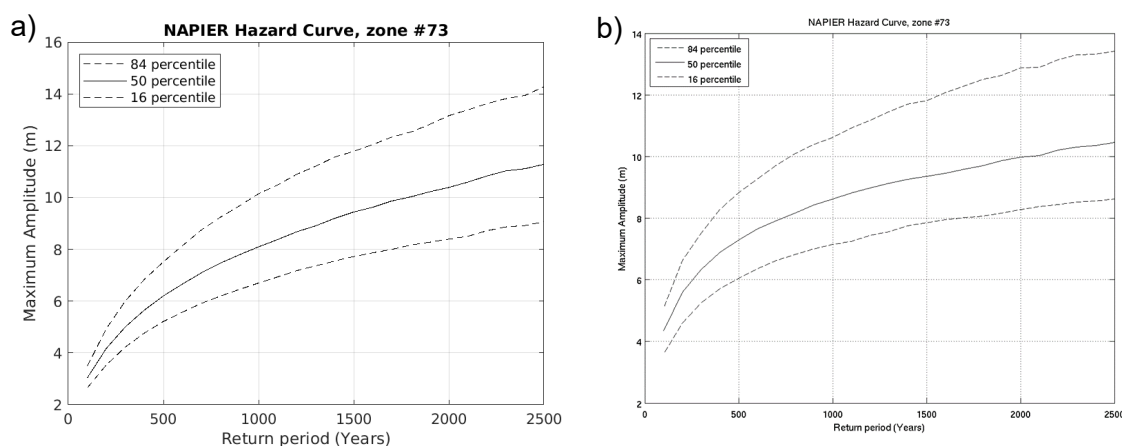


Figure 2.1 Tsunami hazard curves for Zone 73 in (left) NTHM2021 and (right) NTHM2013. The offshore tsunami height (i.e. amplitude in the figure) above mean sea level is a function of the return period.

The hazard at any particular return period usually comes from a range of different earthquake sources. To determine this, we use a process known as 'deaggregation' to determine which sources from a database of scenarios contribute most of the hazard for a specific zone at a given return period. Tables 2.1 and 2.2 show the top six hazard source scenarios at each of the four return periods for Zone 73 and 74, respectively. These sources encompass the majority of the hazard for that particular return period in these zones. The locations of the earthquake sources referred to in the tables are shown in Figure 2.2.

Table 2.1 The top six scenarios and their effective magnitudes for Zone 73 (Napier) determined by deaggregating NTHM2021 (Power et al. 2022) at four return periods: 100, 500, 1000 and 2500 years. Effective magnitude is described in detail in Power (2013). 'SZ' is short for subduction zone. The other sources are crustal faults. The first three deaggregations (return periods 100, 500 and 1000 years) were calculated at the median (50th percentile) hazard value in Zone 73, while the 2500-year one was calculated at the 84th percentile. 'Tsunami Height' is the maximum amplitude of the tsunami in Zone 73 at the corresponding return period and confidence level. 'Weight' is the percentage that this subduction zone or fault contributes to this particular hazard value. Note that only the top six sources are shown, so weights do not add to 100%.

	Return Period (Years)	100	500	1000	2500
	Confidence Level (Percentile)	50	50	50	84
	Tsunami Height in NTHM2021 (m)	3.0	6.2	8.1	14.2
Scenario 1	SZ Name and Weight	Hikurangi SZ 32.2%	Hikurangi SZ 42.2%	Hikurangi SZ 42.9%	Hikurangi SZ 34.4%
	Magnitude Range and Median (Effective M_w)	8.0–8.7, with median of 8.3	8.3–8.9, with median of 8.6	8.5–9.0, with median of 8.7	8.5–9.2, with median of 9.0
Scenario 2	SZ or Fault Name and Weight	Peru SZ 11.5%	Hawkes Bay Outer Rise Fault 6.9%	Hawkes Bay Outer Rise Fault 10.8%	Hawkes Bay Outer Rise Fault 20.8%
	Magnitude Range and Median (Effective M_w)	9.1–9.5, with median of 9.3	8.1–8.1, with median of 8.1	8.2–8.3, with median of 8.2	8.2–8.6, with median of 8.5
Scenario 3	SZ or Fault Name and Weight	North Chile SZ 9.6%	Lachlan Fault 6.8%	North Wairarapa Outer Rise Fault 9.7%	North Wairarapa Outer Rise Fault 16.8%
	Magnitude Range and Median (Effective M_w)	9.0–9.4, with median of 9.2	7.7–7.8, with median of 7.8	8.2–8.3, with median of 8.3	8.2–8.6, with median of 8.5
Scenario 4	SZ or Fault Name and Weight	Kermadec SZ 8.0%	Kermadec SZ 6.6%	Lachlan Fault 7.9%	Lachlan Fault 9.1%
	Magnitude Range and Median (Effective M_w)	8.6–9.3, with median of 8.8	9.0–9.7, with median of 9.3	7.9–7.9, with median of 7.9	7.9–8.2, with median of 8.2
Scenario 5	SZ or Fault Name and Weight	Central Chile SZ 7.3%	North Wairarapa Outer Rise Fault 6.3%	South Wairarapa Outer Rise Fault 5.1%	South Wairarapa Outer Rise Fault = 5.7%
	Magnitude Range and Median (Effective M_w)	9.3–9.7, with median of 9.5	8.1–8.2, with median of 8.1	8.4–8.5, with median of 8.4	8.5–8.8, with median of 8.7
Scenario 6	SZ or Fault Name and Weight	Kuriles-Kamchatka SZ 4.0%	Peru SZ 6.3%	Peru SZ 4.0%	Napier_1931 Fault 2.9%
	Magnitude Range and Median (Effective M_w)	9.3–9.6, with median of 9.4	9.5–9.8, with median of 9.6	9.6–9.9, with median of 9.7	7.9–8.3, with median of 8.2

Table 2.2 The top six scenarios and their effective magnitudes for Zone 74 (Cape Kidnappers) determined by deaggregating NTHM2021 (Power et al. 2022) at four return periods: 100, 500, 1000 and 2500 years. Effective magnitude is described in detail in Power (2013). 'SZ' is short for subduction zone. The other sources are crustal faults. The first three deaggregations (return periods 100, 500 and 1000 years) were calculated at the median hazard value (50th percentile) in Zone 74, while the 2500-year one was calculated at the 84th percentile. 'Tsunami Height' is the maximum amplitude of the tsunami in Zone 74 at the corresponding return period and confidence level. 'Weight' is the percentage that this subduction zone contributes to this particular hazard value. Note that only the top six sources are shown, so weights do not add to 100%.

	Return Period (Years)	100	500	1000	2500
	Confidence Level (Percentile)	50	50	50	84
	Tsunami Height in NTHM 2021 (m)	3.3	6.8	8.9	15.1
Scenario 1	SZ Name and Weight	Hikurangi SZ 38.2%	Hikurangi SZ 39.3%	Hikurangi SZ 42.3%	Hikurangi SZ 33.3%
	Magnitude Range and Median (Effective M_w)	7.9 to 8.7, with median of 8.3	8.4 to 8.9, with median of 8.6	8.5 to 9.0, with median of 8.7	8.6 to 9.2, with median of 9.0
Scenario 2	SZ or Fault Name and Weight	Peru SZ 12.7%	Peru SZ 7.9%	North Wairarapa Outer Rise Fault 9.8%	North Wairarapa Outer Rise Fault 20.5%
	Magnitude Range and Median (Effective M_w)	9.2 to 9.5, with median of 9.3	9.4 to 9.8, with median of 9.5	8.2 to 8.2, with median of 8.2	8.2 to 8.5, with median of 8.4
Scenario 3	SZ or Fault Name and Weight	Central Chile SZ 7.1%	North Wairarapa Outer Rise Fault 6.9%	Hawkes Bay Outer Rise Fault 9.3%	Hawkes Bay Outer Rise Fault 16.6%
	Magnitude Range and Median (Effective M_w)	9.3 to 9.7, with median of 9.4	8.1 to 8.1, with median of 8.1	8.3 to 8.4, with median of 8.3	8.4 to 8.6, with median of 8.6
Scenario 4	SZ or Fault Name and Weight	North Chile SZ 6.5%	Hawkes Bay Outer Rise Fault 6.8%	Lachlan Fault 6.3%	Lachlan Fault 6.9%
	Magnitude Range and Median (Effective M_w)	9.0 to 9.5, with median of 9.2	8.2 to 8.2, with median of 8.2	7.9 to 8.0, with median of 8.0	8.0 to 8.3, with median of 8.2
Scenario 5	SZ or Fault Name and Weight	Kermadec SZ 5.1%	Lachlan Fault 6.3%	Peru SZ 5.3%	South Wairarapa Outer Rise Fault 6.2%
	Magnitude Range and Median (Effective M_w)	8.7 to 9.4, with median of 9.0	7.8 to 7.9, with median of 7.9	9.5 to 9.9, with median of 9.6	8.5 to 8.8, with median of 8.7
Scenario 6	SZ or Fault Name and Weight	Kuriles-Kamchatka SZ 3.5%	Kermadec SZ 4.7%	South Wairarapa Outer Rise Fault 4.7%	Motuokura Fault 4.7%
	Magnitude Range and Median (Effective M_w)	9.3 to 9.6, with median of 9.4	9.1 to 9.7, with median of 9.3	8.4 to 8.5, with median of 8.4	7.9 to 8.2, with median of 8.1

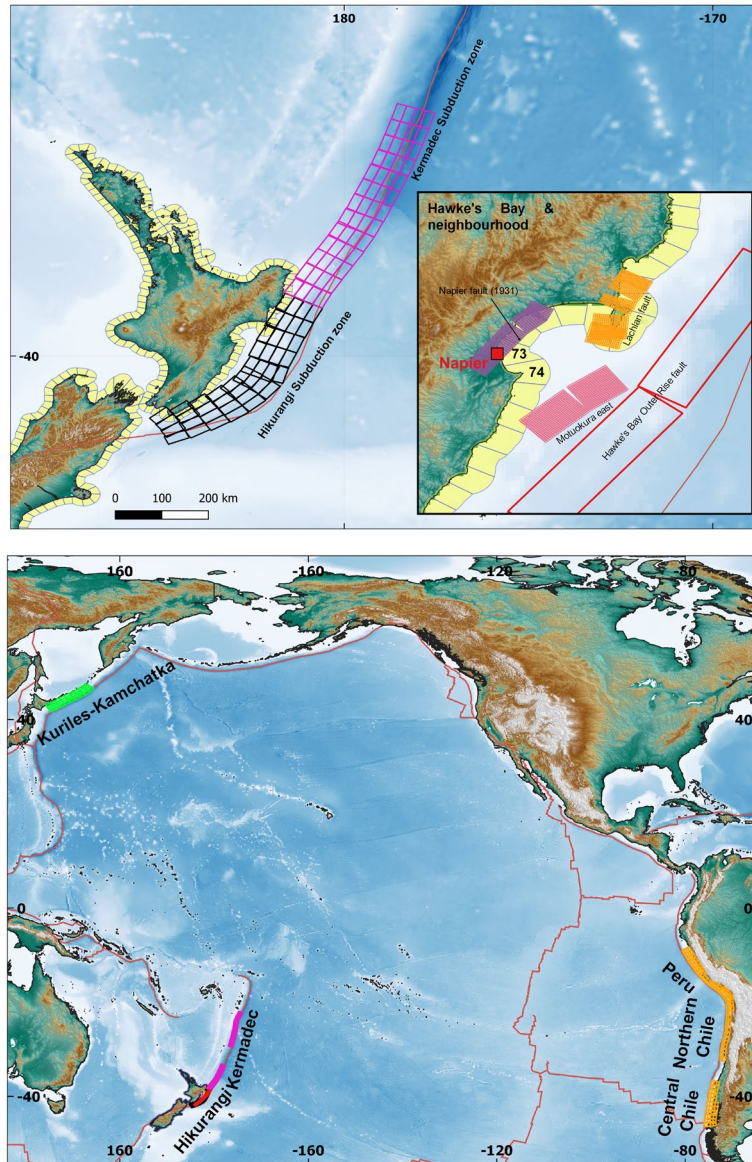


Figure 2.2 Maps showing the location of the faults for each of the scenarios listed in Tables 2.1 and 2.2. Top: the local faults and tsunami zones 73 (Napier) and 74 (Cape Kidnappers). The black and pink squares show the unit sources on each subduction zone. The earthquake used in the simulations was constructed by adding together the deformation from each of these smaller unit sources. Bottom: the distant and regional sources used in this study. The green and orange squares show the unit sources used for the Kurils and South American subduction zone sources, respectively. In addition to the faults shown here, tsunamis from the North and South Wairarapa Outer Rise Faults were also simulated. These faults extend from the 'Hawke's Bay Outer Rise Fault' shown in the top figure down to approximately Cook Strait and run roughly parallel to the Hikurangi subduction zone. They are not shown in regional scale figure to avoid obscuring the Hikurangi Interface unit sources (i.e. the black squares).

As can be seen from Tables 2.1 and 2.2, the tsunami hazard in the two zones is quite similar in terms of tsunami height and the main subduction zones and faults that contribute to it. This means that we can extend the hazard into part of Zone 74 with only a small number of additional scenarios. The scenarios needed for the probabilistic modelling are listed in Table 2.3. This table was compiled by comparing the scenarios in Tables 2.1 and 2.2 and the locations of the specific scenarios. If the median magnitude of the scenario for Zone 73 is within 0.1 magnitude unit of that for the corresponding Zone 74 scenario, and the location of the closest scenario to the target is within a fault length, then we assume that the same scenario can reasonably be used for both coastal zones. The process of selecting the exact location for each scenario along its source is described in detail in Section 2.2. As most of the area of interest is in Zone 73, the magnitude used for the scenario in the modelling stage described in Section 4

will be the median magnitude for Zone 73. If the median of the corresponding scenario is 0.2 magnitude units or more different, or if there is no corresponding scenario for the other coastal zone set or if the closest scenario is more than one fault length away, then we need to model both scenarios. In all, 31 different scenarios need to be modelled through to inundation in Stage 3.

Table 2.3 The 31 scenarios, their effective magnitudes and the return periods used in this study. The final column indicates whether the scenario will be used for both coastal zones or just one. Note that the final hazard maps will not cover the whole of Zone 74, just up to point 2 indicated in Figure 1.1.

Subduction Zone or Fault Name	Effective Magnitude	Return Period (Years)	Used for Coastal Zones:
Hikurangi subduction zone	8.3	100	73
Hikurangi subduction zone	8.3	100	74
Hikurangi subduction zone	8.6	500	73, 74
Hikurangi subduction zone	8.7	1000	73, 74
Hikurangi subduction zone	9.0	2500	73
Hikurangi subduction zone	9.0	2500	74
Peru subduction zone	9.3	100	73
Peru subduction zone	9.3	100	74
Peru subduction zone	9.6	500	73, 74
Peru subduction zone	9.7	1000	73
Peru subduction zone	9.6	1000	74
Central Chile subduction zone	9.5	100	73, 74
North Chile subduction zone	9.2	100	73
North Chile subduction zone	9.2	100	74
Kermadec subduction zone	8.9	100	73, 74
Kermadec subduction zone	9.3	500	73
Kermadec subduction zone	9.3	500	74
Kuriles-Kamchatka	9.4	100	73, 74
Hawkes Bay Outer Rise Fault	8.1	500	73, 74
Hawkes Bay Outer Rise Fault	8.2	1000	73, 74
Hawkes Bay Outer Rise Fault	8.5	2500	73, 74
Lachlan Fault	7.8	500	73, 74
Lachlan Fault	7.9	1000	73, 74
Lachlan Fault	8.2	2500	73, 74
North Wairarapa Outer Rise Fault	8.1	500	73, 74
North Wairarapa Outer Rise Fault	8.3	1000	73, 74
North Wairarapa Outer Rise Fault	8.5	2500	73, 74
South Wairarapa Outer Rise Fault	8.4	1000	73, 74
South Wairarapa Outer Rise Fault	8.7	2500	73, 74
Napier_1931	8.2	2500	73
Motuokura East	8.1	2500	74

2.2 Determining the Earthquake Source Parameters

In order to determine the exact earthquake source parameters (e.g. the exact location of the earthquake along the interface) of each of the scenarios selected for the tsunami inundation modelling, we first found a scenario in the Tsunami Threat Map database (Gusman et al. 2019b) that produced a tsunami height in Tsunami Hazard Zone 73 or 74 closest to the tsunami height (target height) of a given return period and that had a magnitude similar to the deaggregated scenario. We then scaled the slip amount based on the tsunami heights of the selected scenario (initial height) and target height. The target height, initial slip amount and re-scaled slip and resulting moment magnitudes for each of four return periods are shown in the following tables (Zone 73: Tables 2.4, 2.5, 2.6, 2.7; 74: Tables 2.8, 2.9, 2.10, 2.11). To calculate the re-scaled slip amount, we multiplied the initial slip amount with the ratio between the target and initial height. The re-scaled slip amount can be used to calculate the re-scaled moment magnitude (M_W) by first re-calculating the scalar seismic moment (mo) while keeping the rigidity and fault area the same as the initial model values, using Equations 2.1 and 2.2.

$$mo = \mu SA \quad \text{Equation 2.1}$$

$$M_W = \frac{2}{3}(\log(mo) - 9.1) \quad \text{Equation 2.2}$$

The assumed rigidity (μ) is 40 GPa for interplate and outer-rise earthquakes and 34.3 GPa for crustal fault earthquakes, while A is the fault area. These values were chosen to be consistent with values used in other studies, such as Gusman et al. (2019b) and Power et al. (2022). The re-scaled slip and magnitudes for all of the deaggregated scenarios are presented in the following tables for each return period. Note that the effective moment magnitudes indicated in each table are median values.

Table 2.4 Deaggregated source scenarios and the re-scaled slip and magnitude amount used in the inundation modelling for the 100-year return period hazard maps for Zone 73. The target heights and magnitude come from the deaggregation of the NTHM for this return period. The initial height and slip amount were found from the closest scenario in the database to the target magnitude and height. The final slip amount and final moment magnitude after re-scaling are shown in the last two columns. These are the values used in the tsunami simulations later in the project.

Source Name	Target Height (m)	Target Effective Moment Magnitude	Initial Height (m)	Initial Slip Amount (m)	Re-Scaled Slip Amount (m)	Re-Scaled Moment Magnitude
Hikurangi	3.03	8.28	3.55	3.47	2.96	8.25
Peru	3.03	9.30	3.32	19.59	17.89	9.27
Northern Chile	3.03	9.17	2.90	19.96	20.85	9.11
Kermadec	3.03	8.84	2.82	13.86	14.93	8.92
Center Chile	3.03	9.46	2.64	28.37	32.55	9.54
Kuril-Kamchatka	3.03	9.43	2.57	15.24	18.02	9.35

Table 2.5 Deaggregated source scenarios and the re-scaled slip and magnitude amount used in the inundation modelling for the 500-year return period hazard maps for Zone 73. The target heights and magnitude come from the deaggregation of the NTHM for this return period. The initial height and slip amount were found from the closest scenario in the database to the target magnitude and height. The final slip amount and final moment magnitude after re-scaling are shown in the last two columns. These are the values used in the tsunami simulations later in the project.

Source Name	Target Height (m)	Target Effective Moment Magnitude	Initial Height (m)	Initial Slip Amount (m)	Re-Scaled Slip Amount (m)	Re-Scaled Moment Magnitude
Hikurangi	6.20	8.56	6.02	5.83	6.00	8.51
Hawkes Bay Outer rise_1002	6.20	8.123	5.78	10.47	11.23	8.22
Lachlan3_231	6.20	7.80	5.19	4.57	5.46	7.75
Kermadec	6.20	9.27	5.03	21.5	26.51	9.16
North Wairarapa Outer rise	6.20	8.14	7.15	10.47	9.08	8.16
Peru	6.20	9.57	5.88	34.58	36.49	9.52

Table 2.6 Deaggregated source scenarios and the rescaled slip and magnitude amount used in the inundation modelling for the 1000-year return period hazard maps for Zone 73. The target heights and magnitude come from the deaggregation of the NTHM for this return period. The initial height and slip amount were found from the closest scenario in the database to the target magnitude and height. The final slip amount and final moment magnitude after re-scaling are shown in the last two columns. These are the values used in the tsunami simulations later in the project.

Source Name	Target Height (m)	Target Effective Moment Magnitude	Initial Height (m)	Initial Slip Amount (m)	Re-Scaled Slip Amount (m)	Re-Scaled Moment Magnitude
Hikurangi	8.09	8.69	8.27	8.82	8.63	8.69
Hawkes Bay Outer rise_1002	8.09	8.24	5.78	10.47	14.66	8.30
North Wairarapa Outer rise_1003	8.09	8.26	7.15	10.47	11.86	8.24
Lachlan3_231	8.09	7.91	5.19	4.57	7.13	7.83
South Wairarapa Outer rise_1004	8.09	8.44	4.66	10.47	18.16	8.36
Peru	8.09	9.68	5.88	34.58	47.63	9.59

Table 2.7 Deaggregated source scenarios and the rescaled slip and magnitude amount used in the inundation modelling for the 2500-year return period hazard map for Zone 73. The target heights and magnitude come from the deaggregation of the NTHM for this return period. The initial height and slip amount were found from the closest scenario in the database to the target magnitude and height. The final slip amount and final moment magnitude after re-scaling are shown in the last two columns. These are the values used in the tsunami simulations later in the project.

Source Name	Target Height (m)	Target Effective Moment Magnitude	Initial Height (m)	Initial Slip Amount (m)	Re-Scaled Slip Amount (m)	Re-Scaled Moment Magnitude
Hikurangi	14.28	8.97	14.27	13.86	13.87	8.90
Hawkes Bay Outer rise_1002	14.278	8.49	5.77	10.47	25.87	8.46
North Wairarapa Outer rise_1003	14.28	8.50	7.15	10.47	20.92	8.40
Lachlan3_231	14.28	8.15	5.19	4.57	12.57	7.99
South Wairarapa Outer rise_1004	14.28	8.68	4.67	10.47	32.04	8.52
Napier 1931_242	14.28	8.21	3.95	4.58	16.55	8.07

Table 2.8 Deaggregated source scenarios and the re-scaled slip and magnitude amount used in the inundation modelling for the 100-year return period hazard maps for Zone 74. The target heights and magnitude come from the deaggregation of the NTHM for this return period. The initial height and slip amount were found from the closest scenario in the database to the target magnitude and height. The final slip amount and final moment magnitude after re-scaling are shown in the last two columns. These are the values used in the tsunami simulations later in the project.

Source Name	Target Height (m)	Target Effective Moment Magnitude	Initial Height (m)	Initial Slip Amount (m)	Re-Scaled Slip Amount (m)	Re-Scaled Moment Magnitude
Hikurangi	3.37	8.26	3.74	3.47	3.13	8.27
Peru	3.37	9.29	3.35	16.63	16.72	9.30
Centre Chile	3.37	9.41	3.97	30.74	26.14	9.45
Northern Chile	3.37	9.18	4.06	30.48	25.32	9.25
Kermadec	3.37	8.99	2.70	13.86	17.29	8.96
Kuril-Kamchatka	3.37	9.41	2.95	15.24	17.42	9.34

Table 2.9 Deaggregated source scenarios and the re-scaled slip and magnitude amount used in the inundation modelling for the 500-year return period hazard maps for Zone 74. The target heights and magnitude come from the deaggregation of the NTHM for this return period. The initial height and slip amount were found from the closest scenario in the database to the target magnitude and height. The final slip amount and final moment magnitude after re-scaling are shown in the last two columns. These are the values used in the tsunami simulations later in the project.

Source Name	Target Height (m)	Target Effective Moment Magnitude	Initial Height (m)	Initial Slip Amount (m)	Re-Scaled Slip Amount (m)	Re-Scaled Moment Magnitude
Hikurangi	6.80	8.59	6.24	5.83	6.35	8.52
Peru	6.80	9.53	5.88	34.58	40.01	9.54
North Wairarapa Outer rise	6.80	8.10	9.60	10.47	7.41	8.10
Hawkes Bay Outer rise_1002	6.80	8.19	5.80	10.47	12.26	8.25
Lachlan3_231	6.80	7.85	4.57	4.57	6.80	7.81
Kermadec	6.80	9.30	4.98	32.27	44.08	9.39

Table 2.10 Deaggregated source scenarios and the re-scaled slip and magnitude amount used in the inundation modelling for the 1000-year return period hazard maps for Zone 74. The target heights and magnitude come from the deaggregation of the NTHM for this return period. The initial height and slip amount were found from the closest scenario in the database to the target magnitude and height. The final slip amount and final moment magnitude after re-scaling are shown in the last two columns. These are the values used in the tsunami simulations later in the project.

Source Name	Target Height (m)	Target Effective Moment Magnitude	Initial Height (m)	Initial Slip Amount (m)	Re-Scaled Slip Amount (m)	Re-Scaled Moment Magnitude
Hikurangi	8.86	8.70	8.97	8.82	8.70	8.70
North Wairarapa Outer rise_1003	8.86	8.21	9.60	10.47	9.65	8.18
Hawkes Bay Outer rise_1002	8.86	8.30	5.80	10.47	15.97	8.32
Lachlan3_231	8.86	7.96	4.57	4.57	8.86	7.89
Peru	8.86	9.63	7.30	31.62	38.37	9.56
South Wairarapa Outer rise_1004	8.86	8.44	4.79	10.47	19.34	8.38

Table 2.11 Deaggregated source scenarios and the re-scaled slip and magnitude amount used in the inundation modelling for the 2500-year return period hazard maps for Zone 74. The target heights and magnitude come from the deaggregation of the NTHM for this return period. The initial height and slip amount were found from the closest scenario in the database to the target magnitude and height. The final slip amount and final moment magnitude after re-scaling are shown in the last two columns. These are the values used in the tsunami simulations later in the project.

Source Name	Target Height (m)	Target Effective Moment Magnitude	Initial Height (m)	Initial Slip Amount (m)	Re-Scaled Slip Amount (m)	Re-Scaled Moment Magnitude
Hikurangi	15.06	8.98	14.53	17.32	17.95	8.91
North Wairarapa Outer rise_1003	15.06	8.44	9.60	10.47	16.41	8.33
Hawkes Bay Outer rise_1002	15.06	8.53	5.80	10.47	27.16	8.48
Lachlan3_231	15.06	8.18	4.57	4.57	15.06	8.05
South Wairarapa Outer rise_1004	15.06	8.66	4.79	10.47	32.88	8.53
MotuokuraE_293	15.06	8.11	4.57	4.57	15.06	8.05

3.0 DIGITAL ELEVATION MODEL CREATION

Three sets of DEM data have been used in this study to meet spatial accuracy and coverage requirements for the simulation of tsunami originating from their sources, travelling through open sea and interacting with the coasts of Hawke's Bay and its surrounding areas.

These DEM datasets are:

- Global DEM data
- New Zealand DEM data, and
- Hawke's Bay DEM data.

These DEM datasets provide elevation information at numerical modelling grids used for the tsunami simulations (see Section 4).

3.1 Global Digital Elevation Model

Global DEM data was developed at a spatial resolution of 2 arc-minutes (~3600 m on the equator and ~2780 m in Napier) using ETOPO2v2 (<https://www.ngdc.noaa.gov/mgg/global/etopo2.html>) as a base model, together with other data. ETOPO2v2 is a 2 arc-minute global relief model of Earth's surface that integrates land topography and ocean bathymetry and is available from the National Centers for Environmental Information of NOAA (National Oceanic and Atmospheric Administration). In addition to this dataset, the New Zealand DEM data was used to update the New Zealand region in the original ETOPO2v2 data for improved data accuracy.

3.2 New Zealand Digital Elevation Model

The New Zealand DEM data was derived from LINZ charts, the Seabed Mapping CMAP, GEBCO 08 (https://www.gebco.net/news_and_media/updated_gebco_08_release.html) and LINZ 8 m elevation datasets. This DEM dataset covers the main islands of New Zealand and their offshore regions at a grid spacing of 10 arc-seconds (~200–250 m in New Zealand).

3.3 Hawke's Bay Digital Elevation Model

For the scope of the project, we have combined the LiDAR data provided to us by HBRC (Jose Beya, pers. comm.) with our existing bathymetry and elevation data to create a new DEM grid for the region suitable for inundation modelling. The DEM vertical reference is set to MSL, which has zero-elevation. Heights in terms of New Zealand Vertical Datum 2016 (NZVD2016) from the original LiDAR DEM obtained from HBRC were related to the local vertical datum Napier 1962 (MSL), using LINZ conversion file: <https://data.linz.govt.nz/layer/53436-napier-1962-to-nzvd2016-conversion/>. Additional digitisation of georeferenced nautical charts in shallow waters offshore Napier, including Napier Port (i.e. chart NZ 5612 Napier Road¹), has been necessary to increase the resolution of the bathymetry near the coast and inside the port (Figure 3.1). LiDAR data provided by the council covers the stopbanks of the rivers but not the river bathymetry itself. Manual work, using both river cross-sections provided by the council and aerial images, was used to construct the river bathymetry. For this project, we have put together a 5 m resolution DEM grid that covers the area of interest by combining the different irregular datasets using a GIS software (Global Mapper, Blue Marble Geographics®). In order to produce

1 <https://data.linz.govt.nz/layer/51406-chart-nz-5612-napier-roads/> and <https://data.linz.govt.nz/layer/51550-chart-nz-5612-napier-roads/>

a regular 10 m resolution grid suitable for further tsunami simulations, we interpolated the 5 m grid using the kriging methodology in the Surfer® software. Note that kriging is a robust and widely used geostatistical interpolation methodology providing generally better results than more traditional techniques (e.g. linear regression, nearest neighbour, inverse distance weighted, etc.) as long as there is a good spatial correlation between the data points; it uses this spatial correlation between the points (i.e. the spatial distribution) to interpolate the values in space using a variogram (e.g. Arun 2013; Ikechukwu et al. 2017).

We then ran some grid-quality test models to ensure that the resulting 10 m resolution modelling grid does not have any strange bathymetric or topographic points leading to instabilities of the model and that the stop banks were suitably contiguous to inhibit tsunami flow appropriately (see Section 4.8). The final 5 m DEM is shown in Figure 3.2. This DEM is provided with the report.



Figure 3.1 Details of the nearshore bathymetry of the digital elevation model (DEM), including Napier Port and the Ahuriri Estuary revealed with slope shading imaging. The figure shows the local slope in degrees. This method of visualising the DEM highlights the parts of the region with steep slope that are most likely to stop or inhibit the tsunami inundation (e.g. Bluff Hill).

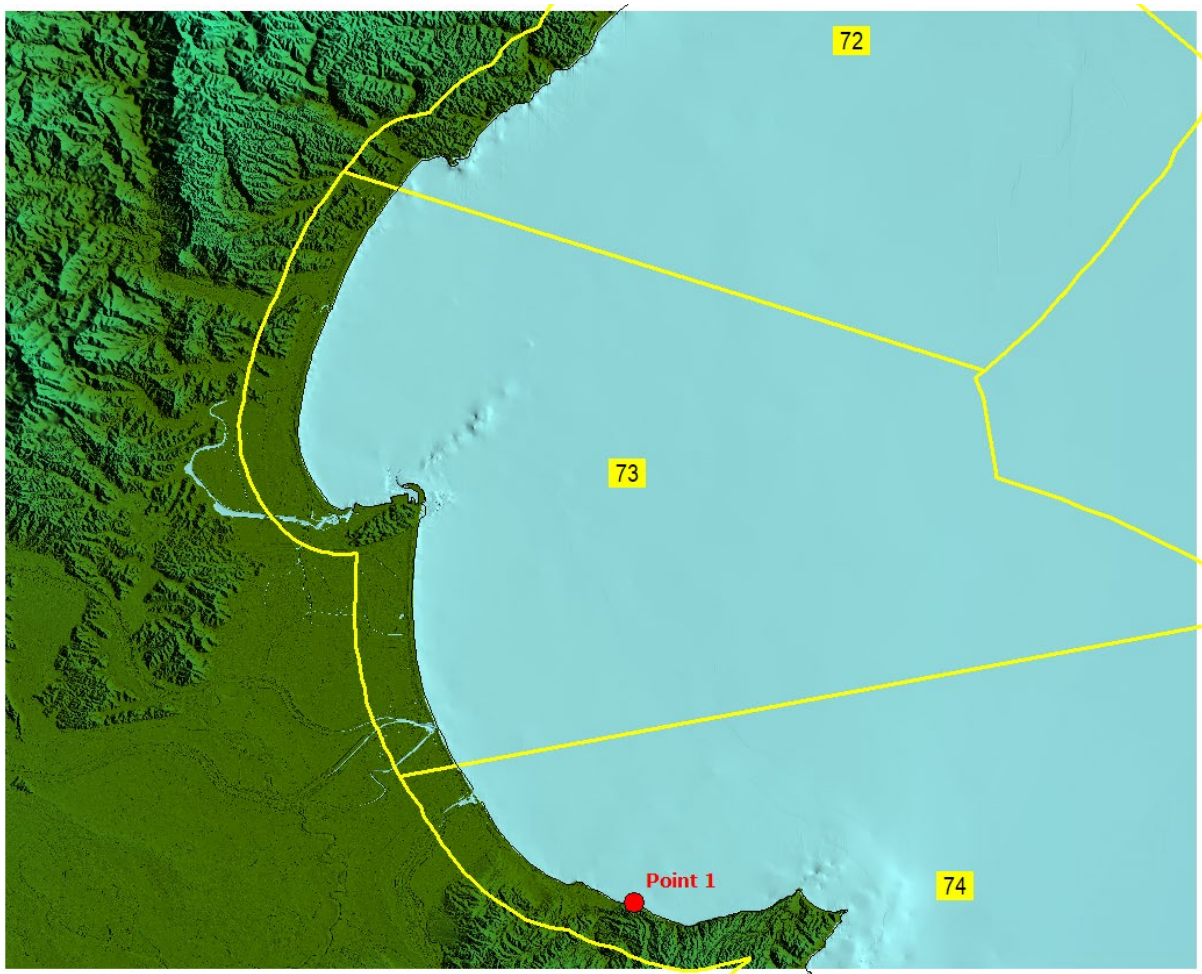


Figure 3.2 The high-resolution (~5 m) DEM created to model the inundation in Zones 73 and part of Zone 74. The yellow lines outline the extents of the tsunami coastal zones; the red dot shows the location of Point 1 as defined in the contract.

4.0 TSUNAMI INUNDATION MODELLING

4.1 Simulation Software: COMCOT

The numerical simulation model, COMCOT (Cornell Multi-grid Coupled Tsunami), was adopted to simulate tsunami generation and propagation from their sources to Hawke's Bay, calculate tsunami evolution inside the bay and model detailed tsunami inundations in its coastal areas. The model was originally developed at Cornell University, USA, in the 1990s (Liu et al. 1998; Wang 2008) and, since 2009, it has been under development at GNS Science, New Zealand (for example, see Wang and Power 2011). Multiple source mechanisms have been integrated in this simulation tool, such as earthquakes with time-dependent rupture, variable slip distributions or landslides.

This model has been widely benchmarked and used by researchers worldwide to study various aspects of tsunami, including tsunami-generation mechanisms, transoceanic propagation, run-up and coastal inundation. In recent years, it has been further developed and is increasingly used to investigate storm surges; wave-structure interactions; effects of rivers, tides and sea-level rise on tsunami hazards; landslides in reservoirs/lakes; and downstream flooding (Wang and Liu 2006; Wijetunge et al. 2008; Beavan et al. 2010; Wang 2008, Wang and Power 2011; Mueller et al. 2015a, 2015b; Wang et al. 2017a, 2017b; Mountjoy et al. 2019; Liu et al. 2018; Li et al. 2018; Mueller et al. 2019; Power et al. 2019; Gusman et al. 2020; Roger et al. 2020; Wang et al. 2020a, 2020b). The latest version of this model was used in this study.

COMCOT uses a modified staggered finite difference scheme to solve linear and non-linear shallow water equations that typically govern tsunami, floods and river flows with shock² capturing up-wind schemes, together with ad-hoc wave breaking algorithms (Kennedy et al. 2000; Lynett 2002; Wang and Power 2011) for improved stability and to account for the energy dissipation effects during run-up and inundation. Both spherical and Cartesian coordinate systems are supported, providing flexibility to tsunami hazard investigations over large transoceanic coverages and small local areas. A two-way nested grid configuration is implemented in the model to balance computational efficiency and numerical accuracy (Wang 2008; Wang and Power 2011). The model uses a relatively large grid spacing to efficiently simulate the propagation of tsunami in the deep ocean and switches to refined grid spacings in near-shore and coastal regions to account for the shortening of tsunami wavelength due to the shallowness of water depth and to achieve sufficient numerical accuracy in the areas of interest (Fraser 2014; Fraser et al. 2014).

4.2 Reference Level and Terminologies

COMCOT uses a universal reference level (zero-elevation level), locally in coincidence with MSL, to interpret input data for elevation information in the DEM and create output data such as tsunami elevations. This reference level is fixed in a virtual space, does not change throughout a numerical simulation and, particularly, is not affected by any potential co-seismic displacements (e.g. uplift or subsidence) in a local earthquake event. During a simulation and

2 This is a modelling method to deal with shock waves in inviscid fluids (common assumption for water for gravity-dominated wave dynamics modelling). Shock waves will lead to a sharp of fluid motions and cause discontinuities of flow variables, a major source of instability. COMCOT uses a conservative form of governing equations so that shock waves become a natural part of the solution. Accuracy and stability are further enhanced by specially designed up-wind finite difference schemes in which no information in front of a shock ('unknown zone') will be used to evaluate derivatives, based on velocity directions.

in output data, 'tsunami elevation' is defined as the tsunami water surface level above the universal reference level (e.g. MSL) and 'tsunami flow depth' refers to the vertical water layer thickness between the water surface and topographical surface (ground or seafloor surface) as defined in the DEM (Figure 3.1). Elevation data is positive if above the universal reference level (in this case, tsunami elevation is often called tsunami height) and negative if below it. Note that flow depth values are independent of reference levels.

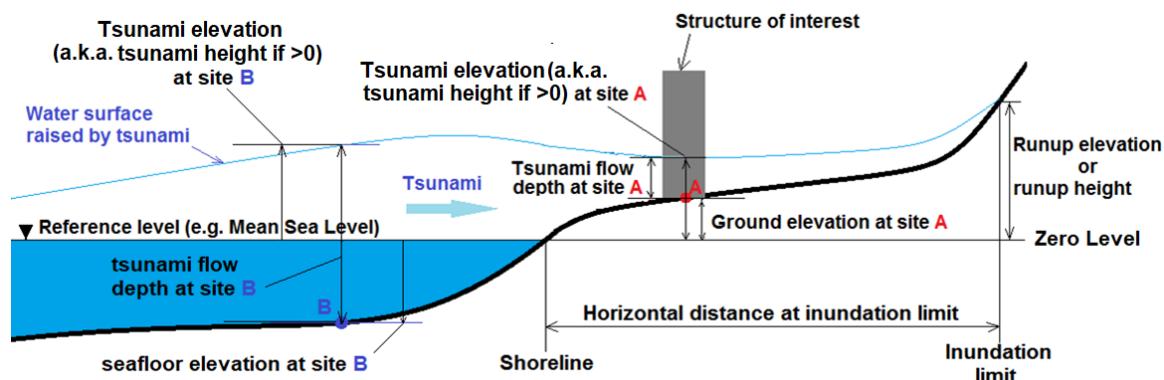


Figure 4.1 Illustration of some definitions used in tsunami modelling, for example, water surface level / tsunami elevation (i.e. tsunami height), tsunami flow depth / inundation depth and ground elevation at site location A on land and B in water.

4.3 Modelling Grid Set-Up

COMCOT uses a series of nested numerical modelling grids at cascading spatial resolutions to account for spatial resolution requirements by a tsunami travelling in different regions, e.g. from deep ocean basin to shallow coastal areas (Wang and Power 2011). In this study, four levels of numerical grid with different spacing refinement were used to simulate tsunami generation, transoceanic propagation, coastal run-up and inundation. This nested grid set-up is able to telescope spatial resolutions from 2 arc-minutes (~3600 m on the Equator), covering the entire Pacific, to 0.5 arc-seconds (about 11 metres) covering the Hawke's Bay and its surrounding areas.

The first grid level (grid 01) covers the whole Pacific Ocean to simulate tsunami generations and propagations from a variety of sources at a spatial resolution of 2 arc-minutes (~3900 m on the Equator and ~2850 m in Napier, see Figure 4.2). The elevation data of grid 01 was interpolated from the Global DEM data described in Section 3.1.

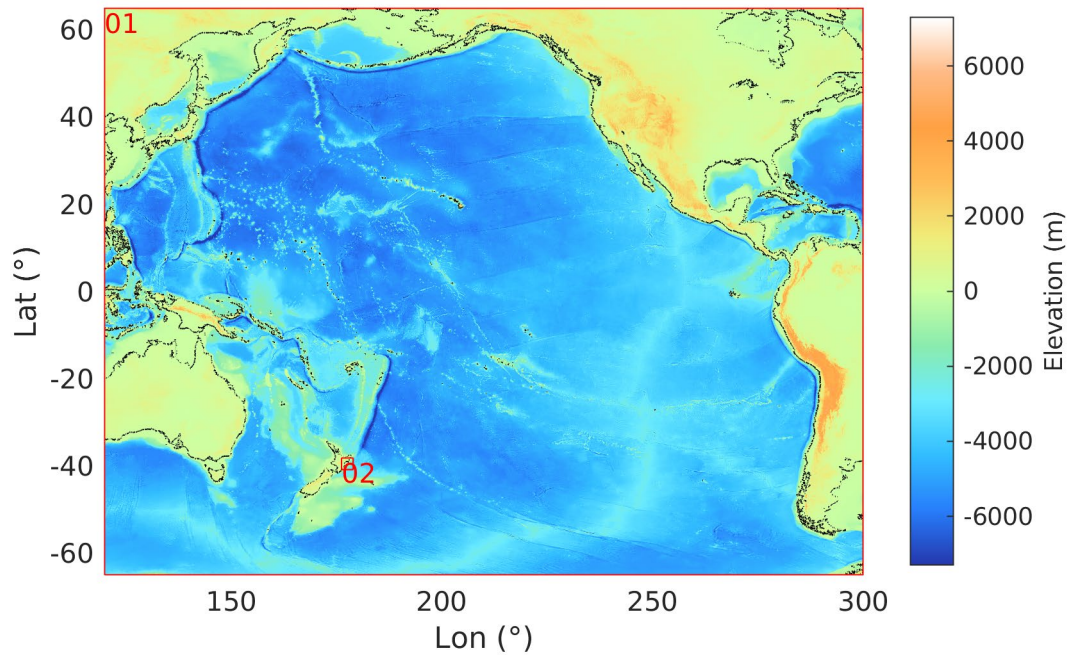


Figure 4.2 Coverage of modelling grid 01 for the Hawke's Bay modelling. Red box outlines the coverage of grid 02. Elevation (relative to MSL) is colour-coded in metres. Data is from the global DEM grids with a spatial resolution of 2 arc-minutes.

The second grid level (grid 02) covers part of New Zealand's North Island east coast at 15 arc-seconds (~310–380 m in New Zealand and ~360 m in Hawke's Bay, see Figures 4.2 and 4.3). The third grid level (grid 03) covers the Hawke's Bay region at a spatial resolution of 1.875 arc-seconds (~45 m in Napier), shown in Figure 4.3. The elevation data of grids 02 and 03 were all interpolated from the 10 arc-second New Zealand DEM data described in Section 3.2.

The fourth and last grid level (grid 04) covers part of the Hawke's Bay region around Napier and its surrounding suburbs and the sea in front of it at a spatial resolution of ~0.47 arc-seconds, which is about 11 m at Napier's latitude (Figure 4.4). Its elevation data was interpolated from the 5 m Hawke's Bay DEM described in Section 3.3. This DEM is also provided with the report.

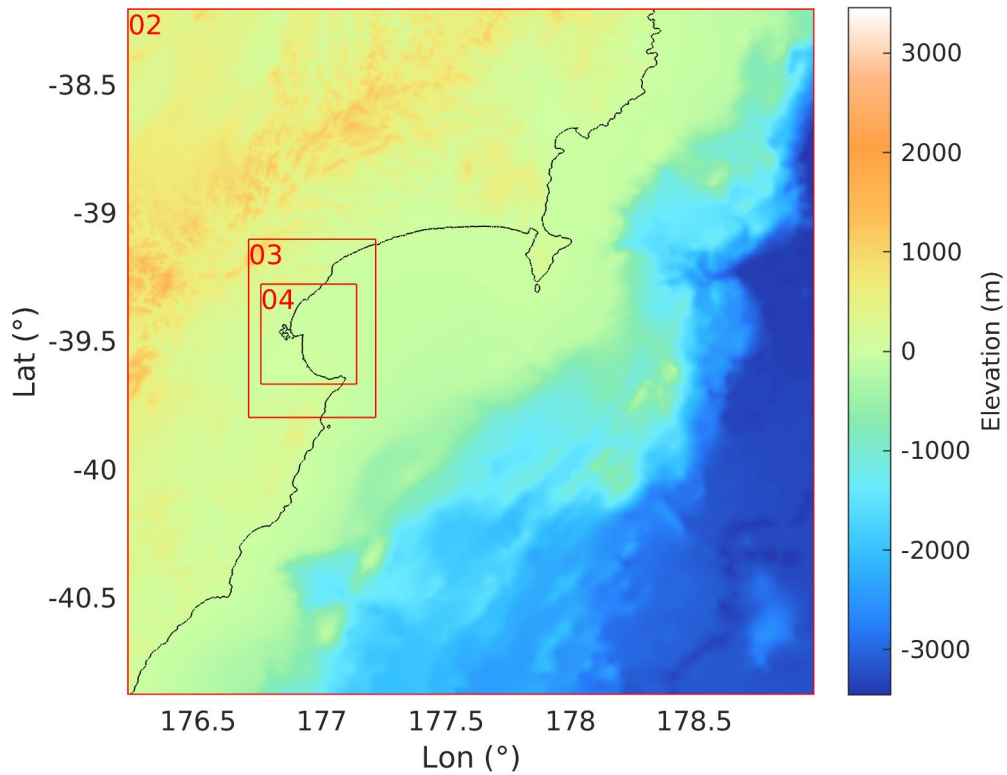


Figure 4.3 Coverage of modelling grid 02. Red boxes show the location of grids 03 and 04. Elevation (relative to MSL) is colour-coded in metres.

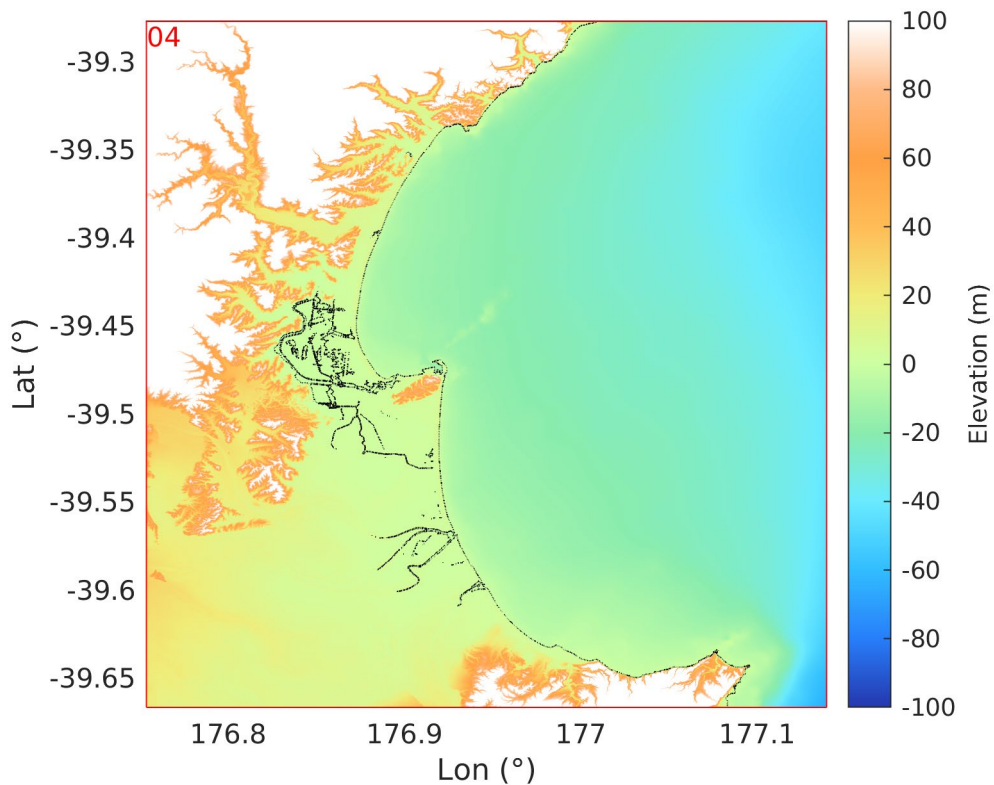


Figure 4.4 Coverage of modelling grid 04, which has the highest level of detail (~11 m) used for the modelling of tsunami inundation in the Hawke's Bay region. Elevation (relative to MSL) is colour-coded in metres. The black contour shows the 0 m contour at MSL.

Table 4.1 summarises the nested grid set-up and modelling settings used for this study.

Table 4.1 Nested grid set-up for tsunami simulations. The grid sizes are indicative and only accurate along parallels of latitude; refer to Section 4.6 for further detail about grid sizes.

Grid	Grid Coverage	Grid Size (Arc-Second)	Time Step (Second)	Tsunami Model	Boundary Condition
01	120.0~300.0E, -65.0~65.0N	120.00 (~2700 m)	3.0885	Linear	Absorbing
02	176.2~179.0, -40.9~-38.2	15.00 (~360 m)	1.0295	Linear	2-way nested
03	176.7~177.22, -39.8~-39.1	1.86 (~45 m)	0.5147	Linear	2-way nested
04	176.7535~177.14, -39.6670~-39.2770	0.47 (~11 m)	0.1715	Non-linear	2-way nested

4.4 Roughness Model

In tsunami inundation modelling, a commonly adopted approach is that land-cover features, such as buildings, are deliberately removed from DEM data and replaced with corresponding equivalent roughness values for different types of land covers to simplify the computation (see Wang et al. 2017a and references therein). It is also preferable that a range of roughness values are used for different land-cover types in an inundation simulation in order to account for the spatial variation of their resistance effects on tsunami flow dynamics.

In this study, we used a set of roughness values (i.e., Manning's roughness coefficient, n ; Manning 1891) for a relatively simplified set of land-cover groups proposed in Wang et al. (2017a). The land-coverage groups and their roughness values are given in Table 4.2. These values were derived by comparing roughness values found in the literature, grouping and averaging roughness values for similar land-cover types (Arcement and Schneider 1984; Fujima 2001; Imamura et al. 2006; Wang and Liu 2007; Wang et al. 2009; Gayer et al. 2010; Kaiser et al. 2011; Fraser et al. 2014; Bricker et al. 2015) but leaning slightly toward the lower end of the value ranges.

Table 4.2 Roughness values for different land-cover groups for the tsunami modelling.

Land-Cover Group	Manning's n (Roughness Coefficient)
Built-up area (e.g. urban / residential / industrial / Central Business District)	0.060
Tall vegetation (e.g. forest)	0.040
Scrub (e.g. low trees / bushes)	0.040
Low vegetation (e.g. grass)	0.030
Urban open area (e.g. paved/smoothed)	0.025
Bare land (e.g. farmland)	0.025
Water area (e.g. riverbed/seabed)	0.011

Figure 4.5 shows the spatial distribution of roughness values (Manning's n) for different land-cover groups in the Hawke's Bay and its surrounding areas. The roughness grid was developed using the land cover data obtained from the LRIS portal (<https://lris.scinfo.org.nz/layer/104400-lcdb-v50-land-cover-database-version-50-mainland-new-zealand/>). The land cover types were grouped into five categories, each was assigned the Manning coefficient n (see Figure 4.5) and the resulting polygons were turned into a grid within ArcGIS software.

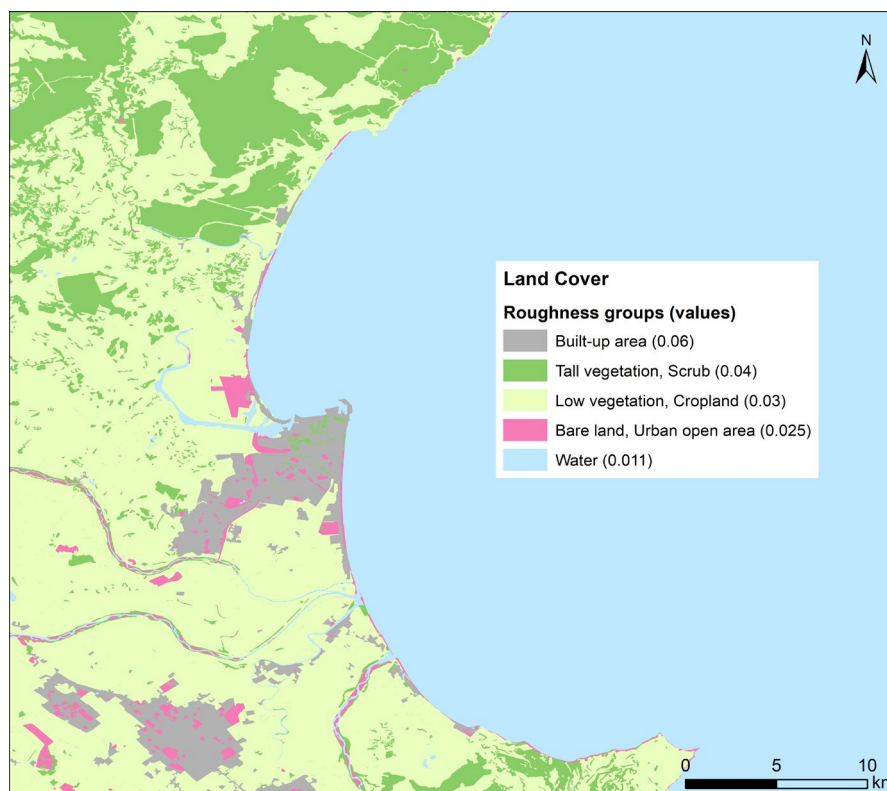


Figure 4.5 Spatial distribution of equivalent surface roughness values, i.e. Manning's n , in Hawke's Bay (grid 04) for tsunami inundation modelling.

4.5 Special Treatment with Low-Lying Dry Land

Special consideration has been made to deal with low-lying areas around the Hawke's Bay airport and to the south of Ahuriri Estuary, as shown in Figure 4.6. These low-lying areas are below MSL, but are actually dry land, not connected to the open sea at MSL. Without special treatment, these areas would appear as 'water' and be modelled as such in numerical simulations of tsunami.

In this modelling, a special algorithm in COMCOT was applied to completely 'drain' the artificial water in these areas. This was achieved by setting initial values of flow depth at numerical grids within these low-lying dry areas to zero before a tsunami simulation starts.

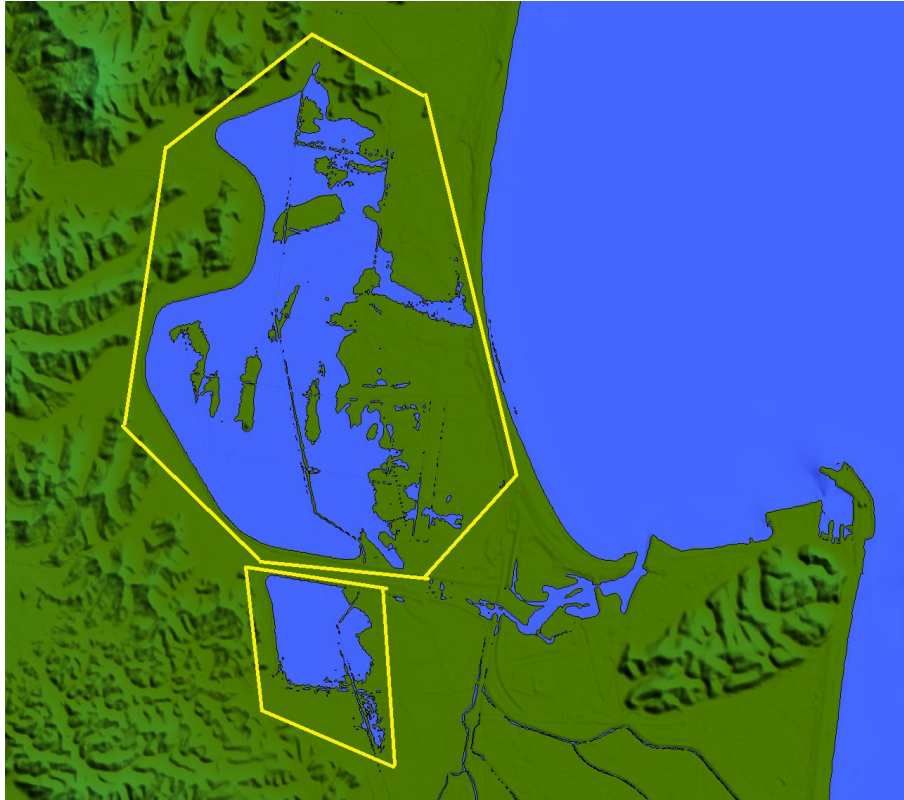


Figure 4.6 Yellow polygons outline low-lying land areas around Hawke's Bay Airport and south of Ahuriri Estuary. These dry land areas are below MSL.

4.6 Effects of Earth Curvature, Rotation and High Latitude

This study adopts tsunami-governing equations in a Spherical Coordinate System to simulate tsunami from selected sources to the Hawke's Bay region. This is necessary for tsunami simulations over a very large area that need to consider the curvature of the Earth's surface. The effect of the Earth's rotation was also evaluated through the inclusion of the Coriolis force in both linear and non-linear tsunami models in COMCOT (Wang and Power 2011).

In high-latitude regions, the commonly used approach of using 'square' grids in spherical coordinates, i.e. equal cell edges in arc-degrees, leads to grid cells that are highly elongated when measured in metres. For example, for this type of grid in Hawke's Bay, the S–N edge of a grid cell will be over 30% longer than its W–E edge. This will not only affect the stability of tsunami simulations but also lead to inconsistent accuracies of modelling results in different directions.

To overcome these issues, the size of a numerical grid cell in COMCOT varies along its meridian (i.e. lines of longitude) and is self-adjusted according to its latitude so that its edge length along the parallel (i.e. circles of latitude) and meridian are equal in metres. This ensures that 'square' grids (in metre terms) are created for numerical calculations and thus maintains the same accuracies in different directions. As a result, the grid sizes given in Table 4.1 are nominal and are only true along the parallels.

4.7 Other Simulation Settings

In the tsunami simulations, co-seismic ground surface and seafloor displacement in an earthquake event is calculated using the widely used elastic finite fault theory of Okada (1985) and is introduced in the model as the initial condition of tsunami generation.

In local earthquake events, the co-seismic uplift or subsidence may also change the ground and seafloor elevation as defined in the input DEM (i.e. current-day or pre-event DEM). When this happens, the COMCOT model firstly adjusts the input DEM with the computed co-seismic uplift/subsidence and then simulates the subsequent tsunami to calculate hazard parameters, e.g. tsunami elevation, flow depth, flow velocity and flow acceleration, over the adjusted DEM (i.e. post-event DEM).

In the numerical simulations, tsunami propagation was simulated for 30 hours for distant scenarios (e.g. South America), 15 hours for regional scenarios (e.g. Kermadec) and 10 for local earthquake scenarios (e.g. Hikurangi and New Zealand crustal faults) from their generation in the sources to ensure that the maximum tsunami hazard parameters were obtained in the Hawke's Bay region. Detailed examinations of selected scenarios revealed that the maximum tsunami inundation extents had clearly been reached in less than 10 hours after first arrivals, assuring that these run times were long enough. All of the simulations assume that tsunami occurs at MHWS or at MHWS plus the appropriate sea-level rise. MHWS was modelled as a static level above the local MSL, not changing over time with the tidal fluctuations.

4.8 Test Runs

To ensure that the DEMs were constructed correctly and that features such as the stopbanks were included correctly, we ran multiple test scenarios using the grid set-up described above. For testing purposes, we used both local and distant earthquake scenarios with uniform and non-uniform slip distributions. One example is shown in Figure 4.6. The stop banks performed as expected across the tests and inhibited the water entering the low-lying areas, including the tsunami flow. This is particularly important to verify at the beginning of the simulation process when we add the sea-level rise value to the actual MSL (Figure 4.7). In the example shown below, 0.92 m (corresponding to MHWS) is added to MSL. If the stopbanks were open, or if a special condition had not been specified for the low-lying areas, then the water would enter these low-lying areas immediately, which is not the case here. This kind of test shows that the stopbanks are contiguous in the model and that COMCOT deals correctly with the low-lying areas with altitude under MSL or MHWS.

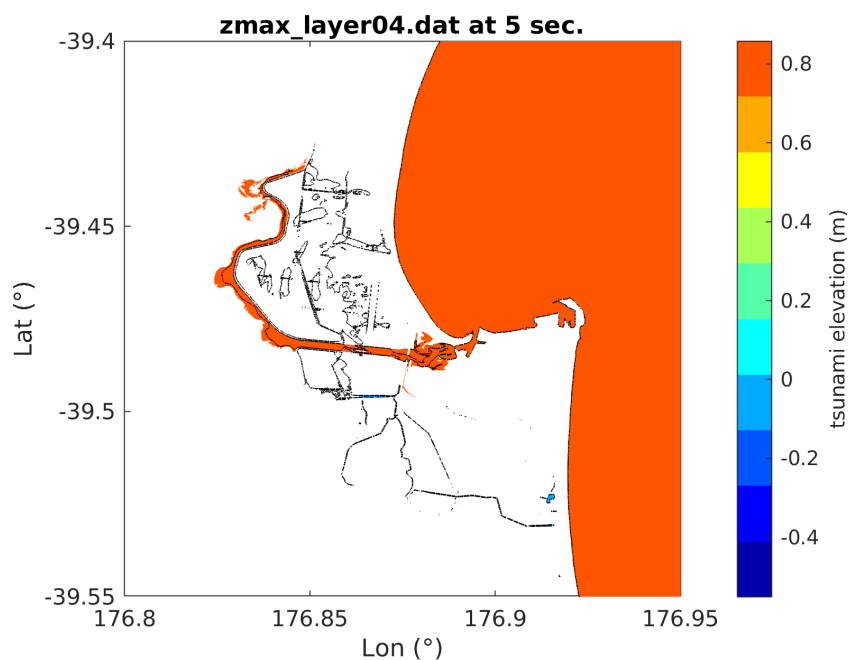


Figure 4.7 Example of the results of one of the test scenarios. Note that the stopbanks (shown as black lines along the waterway) inhibit the water to enter the low-lying areas, especially the one around Hawke's Bay airport at MHWS (+92 cm) at the beginning of the simulation (shown in the figure with a tsunami propagation time of 5 seconds).

4.9 Final Models

For each of the scenarios indicated in Section 2, we ran the models through all of the grids to inundation on the last level (grid 05). An example of one of them is shown in Figure 4.8. It shows the inundation produced by a M_w 8.9 earthquake on the Hikurangi subduction zone. This was one of the scenarios that contributed to the hazard at a return period of 2500 years and is the largest contributor to the hazard for this return period. This particular scenario also causes one of the largest amounts of inundation to Napier, along with the Napier crustal fault and the Hawkes Bay Outer Rise Fault in NTHM2021 at the current MHWS.

Flow depth Hawke's Bay (grid04) - 04_PERIOD_2500yr - Hiku-Ker_Pt3_Mw8.90
Maximum flow depth = 16.0294 m

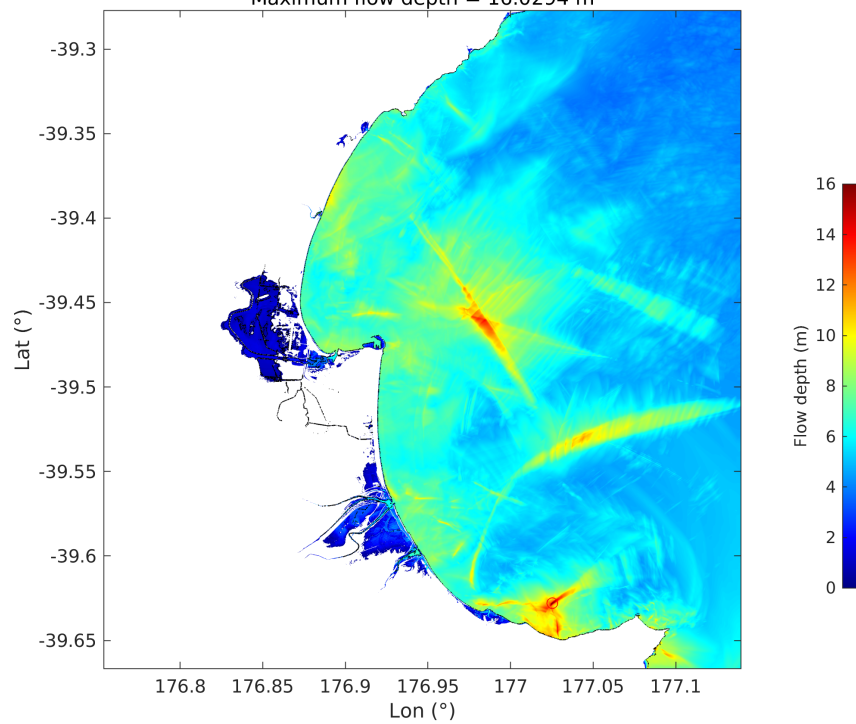


Figure 4.8 Example of the inundation produced from a Mw 8.9 event on the Hikurangi subduction zone at MHWS for a return period of 2500 years. Onshore values refer to flow depths, while offshore values refer to maximum tsunami heights.

5.0 PROBABILISTIC TSUNAMI INUNDATION HAZARD MAPS

The contribution of each of the inundation scenarios were then normalised according to their contribution to the hazard (the pre-normalised values are the 'weights' in Tables 2.1 and 2.2). The exact weights are shown in Tables 5.1 and 5.2 for each coastal zone. As we have two sets of weights (one for Zone 73 and 74), we have sets of maps for each combination of return period and sea-level rise. The resulting maps of median and 84th percentile flow depths/heights are shown in Figures 5.2–5.17 following the tables.

Table 5.1 Scenario normalised contribution for Zone 73.

Annual Probability of Exceedance	Source Name	Effective Magnitude	Percentage of Deaggregation	Percentage of Top Sources ('Normalised')
1:100	Hikurangi	8.28	32.18	44.40
1:100	Peru	9.30	11.50	15.87
1:100	Northern Chile	9.17	9.55	13.18
1:100	Kermadec	8.84	8.02	11.06
1:100	Center Chile	9.46	7.25	10.00
1:100	Kuril-Kamchatka	9.44	3.98	5.50
1:500	Hikurangi	8.56	42.18	56.09
1:500	Hawkes Bay Outer rise_1002	8.13	6.92	9.20
1:500	Lachlan3_231	7.80	6.82	9.06
1:500	Kermadec	9.26	6.63	8.82
1:500	North Wairarapa Outer rise	8.14	6.33	8.42
1:500	Peru	9.57	6.32	8.40
1:1000	Hikurangi	8.69	42.93	53.41
1:1000	Hawkes Bay Outer rise_1002	8.24	10.80	13.44
1:1000	North Wairarapa Outer rise_1003	8.26	9.65	12.00
1:1000	Lachlan3_231	7.91	7.85	9.77
1:1000	South Wairarapa Outer rise_1004	8.44	5.12	6.37
1:1000	Peru	9.68	4.03	5.02
1:2500	Hikurangi	8.97	34.37	38.29
1:2500	Hawkes Bay Outer rise_1002	8.49	20.83	23.21
1:2500	North Wairarapa Outer rise_1003	8.50	16.83	18.76
1:2500	Lachlan3_231	8.15	9.12	10.16
1:2500	South Wairarapa Outer rise_1004	8.68	5.73	6.39
1:2500	Napier 1931_242	8.21	2.87	3.19

Table 5.2 Scenario normalised contribution for Zones 74.

Annual Probability of Exceedance	Source Name	Effective Magnitude	Percentage of Deaggregation	Percentage of Top Sources ('Normalised')
1:100	Hikurangi	8.26	38.28	52.37
1:100	Peru	9.29	12.70	17.37
1:100	Center Chile	9.41	7.08	9.69
1:100	Northern Chile	9.18	6.47	8.85
1:100	Kermadec	8.99	5.12	7.00
1:100	Kuril-Kamchatka	9.41	3.45	4.72
1:500	Hikurangi	8.59	39.25	54.63
1:500	Peru	9.54	7.90	11.00
1:500	North Wairarapa Outer rise	8.10	6.90	9.60
1:500	Hawkes Bay Outer rise_1002	8.19	6.78	9.44
1:500	Lachlan3_231	7.85	6.30	8.77
1:500	Kermadec	9.30	4.72	6.56
1:1000	Hikurangi	8.70	42.30	54.53
1:1000	North Wairarapa Outer rise_1003	8.22	9.78	12.61
1:1000	Hawkes Bay Outer rise_1002	8.30	9.27	11.95
1:1000	Lachlan3_231	7.96	6.25	8.06
1:1000	Peru	9.63	5.27	6.79
1:1000	South Wairarapa Outer rise_1004	8.44	4.70	6.06
1:2500	Hikurangi	8.98	33.27	37.79
1:2500	North Wairarapa Outer rise_1003	8.44	20.50	23.29
1:2500	Hawkes Bay Outer rise_1002	8.53	16.55	18.80
1:2500	Lachlan3_231	8.18	6.85	7.78
1:2500	South Wairarapa Outer rise_1004	8.66	6.22	7.06
1:2500	MotuokuraE_293	8.11	4.65	5.28

As expected, at the 100-year return period, the extent of inundation is small at the current MHS, restrained to the low-lying area around the airport and immediate neighbourhood of waterways. However, at the 1000- and 2500-year return periods, the inundation extents are much larger, with most of the inundation occurring in Napier's coastal suburbs of Ahuriri and Awatoto, the low-lying area around the Hawke's Bay Airport, Napier Port and small towns south of the Tutaekuri river (i.e. Clive, Haumoana and Te Awanga).

One other point to note is that the inundation extents for the Zone 73 scenarios are almost the same as those for the Zone 74 scenarios for all return periods and sea-level rise values considered here. This is a consequence of the deaggregation, which showed that the main source of tsunami hazard for most zones is similar. However, there are some minor differences in a few areas, particularly at the 100-year return period. As a result, ***we recommend that HBRC use the Zone 73 map for the coastal strip in Zone 73 and that the Zone 74 maps are used for the area out to point 1 (Figure 3.2) within that coastal zone.***

The effect of adding 0.65 m, 1 m or 1.99 m of sea-level rise projections is equivalent to increase the area inundated at a given return period. For example, adding 1.99 m of sea-level rise to the model increases the area inundated by the 1:100-year tsunami (Figure 5.4) beyond that inundated by the 1:2500 event at MHWS (Figure 5.13). Increasing the sea-level by these large amounts has a greater impact on the area inundated than increasing the return period within this range. Note also that the figures show the inundation caused by the sea-level rise combined with that caused by the tsunami. We have illustrated the effect of the sea-level rise component by itself in Figure 5.1(a–c). The effect of the sea-level rise is that the low-lying areas of the coast start the simulation inundated by the sea-level rise before the tsunami even arrives. This occurs in the areas between the black contour line and the other white, green or red lines, depending on the sea-level rise amount. The flow depths shown in Figures 5.2–5.17 include both this effect and the maximum flow depth of the subsequent tsunami. In other words, the flow depths in the hazard maps show the inundation depths caused by both the sea-level rise component and subsequent tsunami put together.

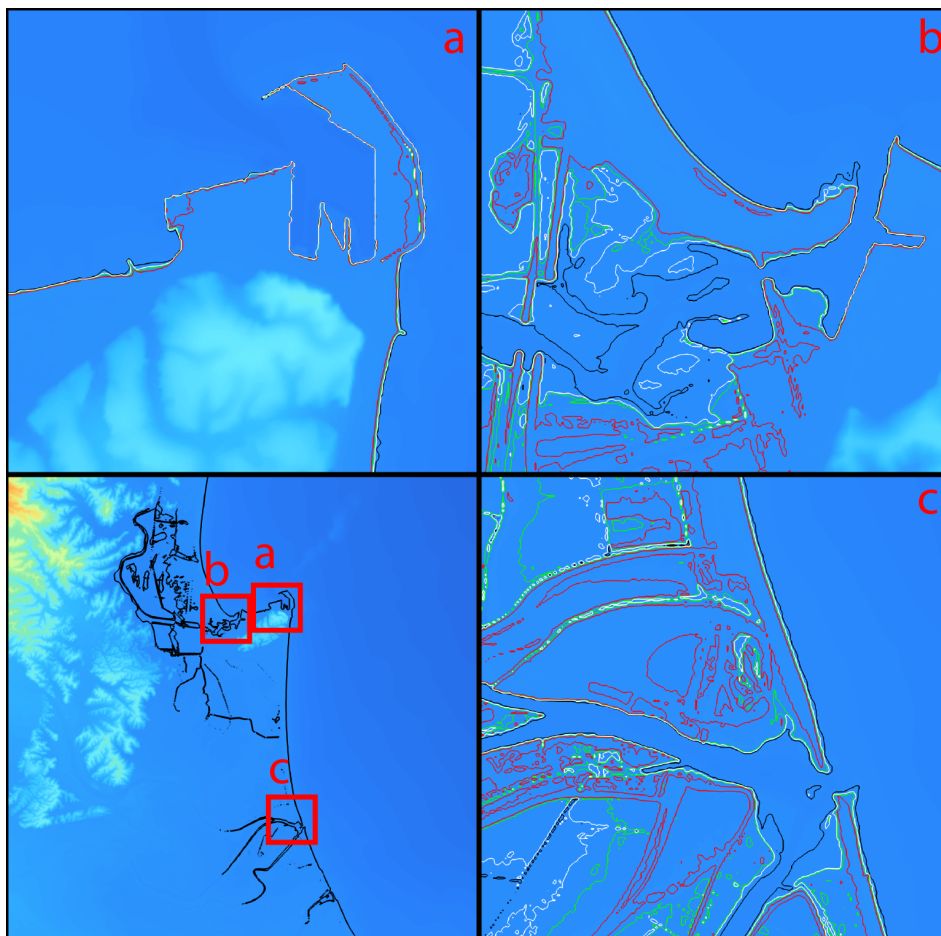


Figure 5.1 The DEM used grid 04 zoomed into (a) Napier Harbour, (b) Ahuriri Estuary and (c) Ngaruroro Estuary. The figure in the bottom left shows the DEM at a regional scale. In parts (a–c), the black line is the 0 m contour at MHWS, the white line is the 0 m contour at MHWS with the additional 0.65 m sea-level rise, the green line is the 0 m contour at MHWS plus an additional 1 m of sea-level rise and the red line is the 0 m contour at MHWS plus 1.99 m of sea-level rise. In some areas, such as those shown in (b) and (c), much of the coastal area is inundated before the tsunami even arrives by the addition of the sea-level rise component. In areas such as (a), the effect is more limited to low-lying areas just near the coast.

The data shown in the maps are provided to HBRC as rasters of the median flow depth/height and feature classes of tsunami inundation extent. All of the datasets are in WGS 1984 geographic coordinate system but are capable of being converted to other projection systems if HBRC chooses to do so.

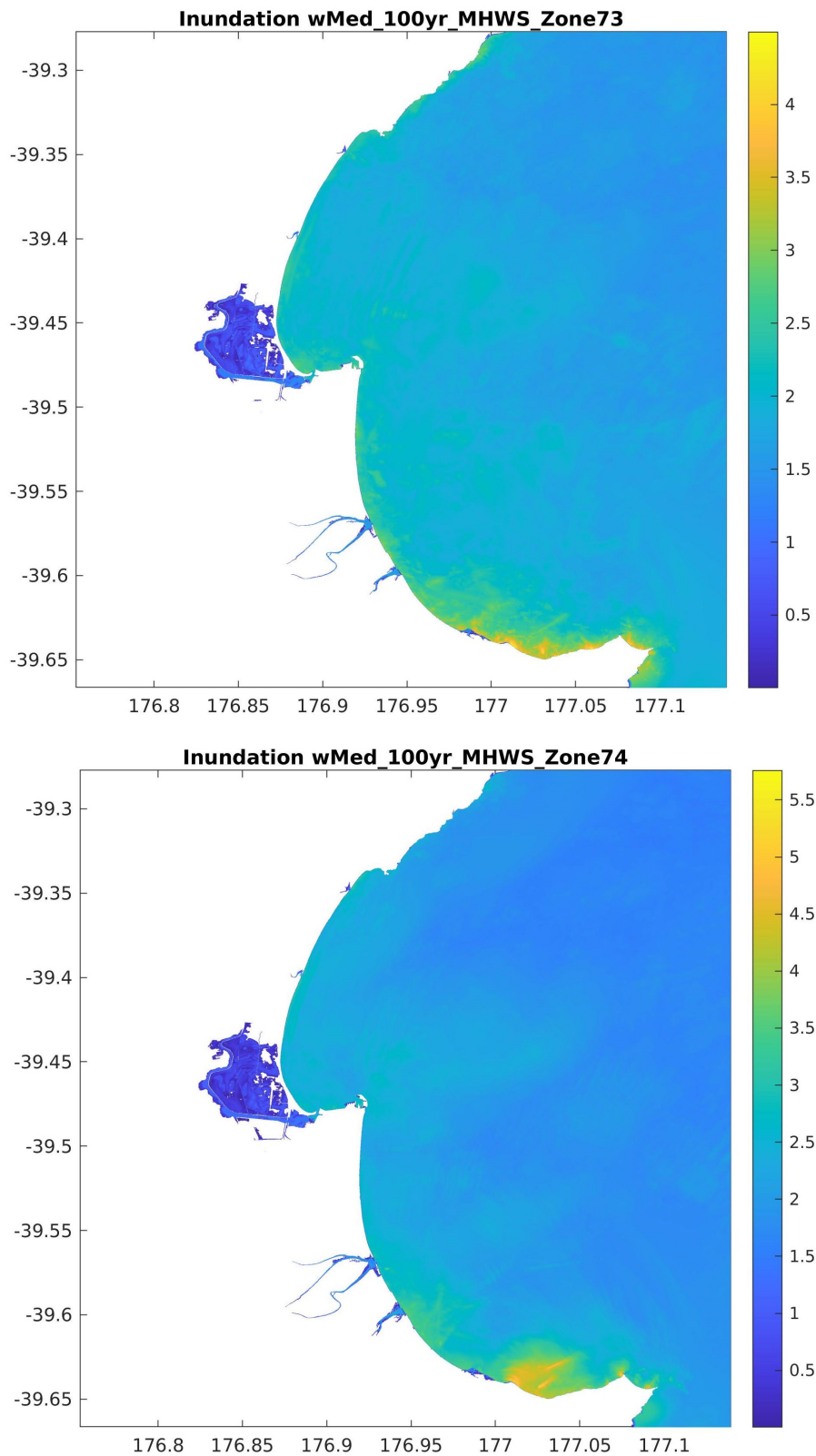


Figure 5.2 Probabilistic tsunami inundation maps for Hawke's Bay showing the median flow depths onshore and offshore tsunami heights with a 1-in-100-years chance of being exceeded per annum at current MHWS. Onshore values refer to flow depths, while offshore values refer to maximum tsunami heights.

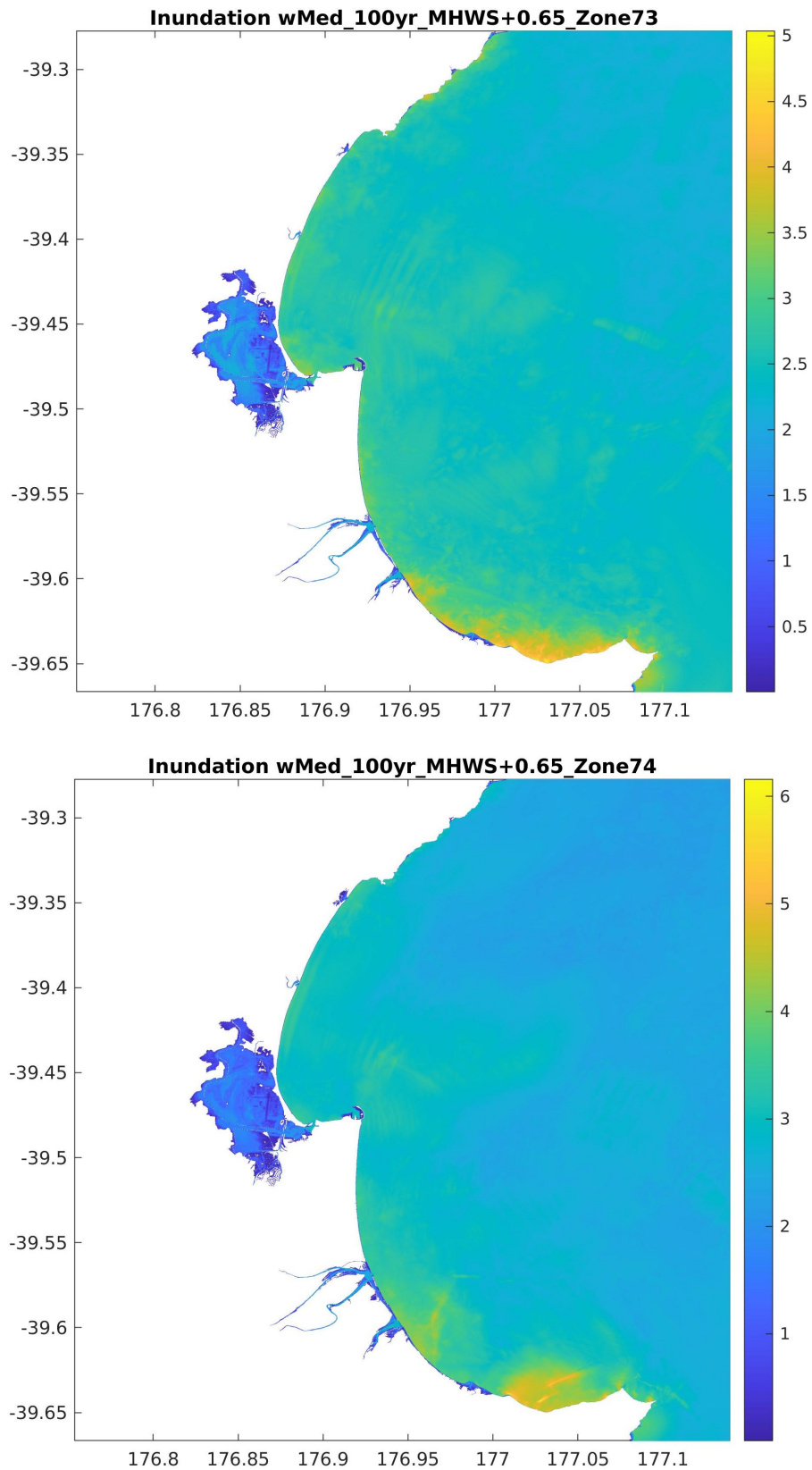


Figure 5.3 Probabilistic tsunami inundation maps for Hawke's Bay showing the median flow depths onshore and offshore tsunami heights with a 1-in-100-years chance of being exceeded per annum at current MHWS plus 0.65 m of sea-level rise. Onshore values refer to flow depths, while offshore values refer to maximum tsunami heights.

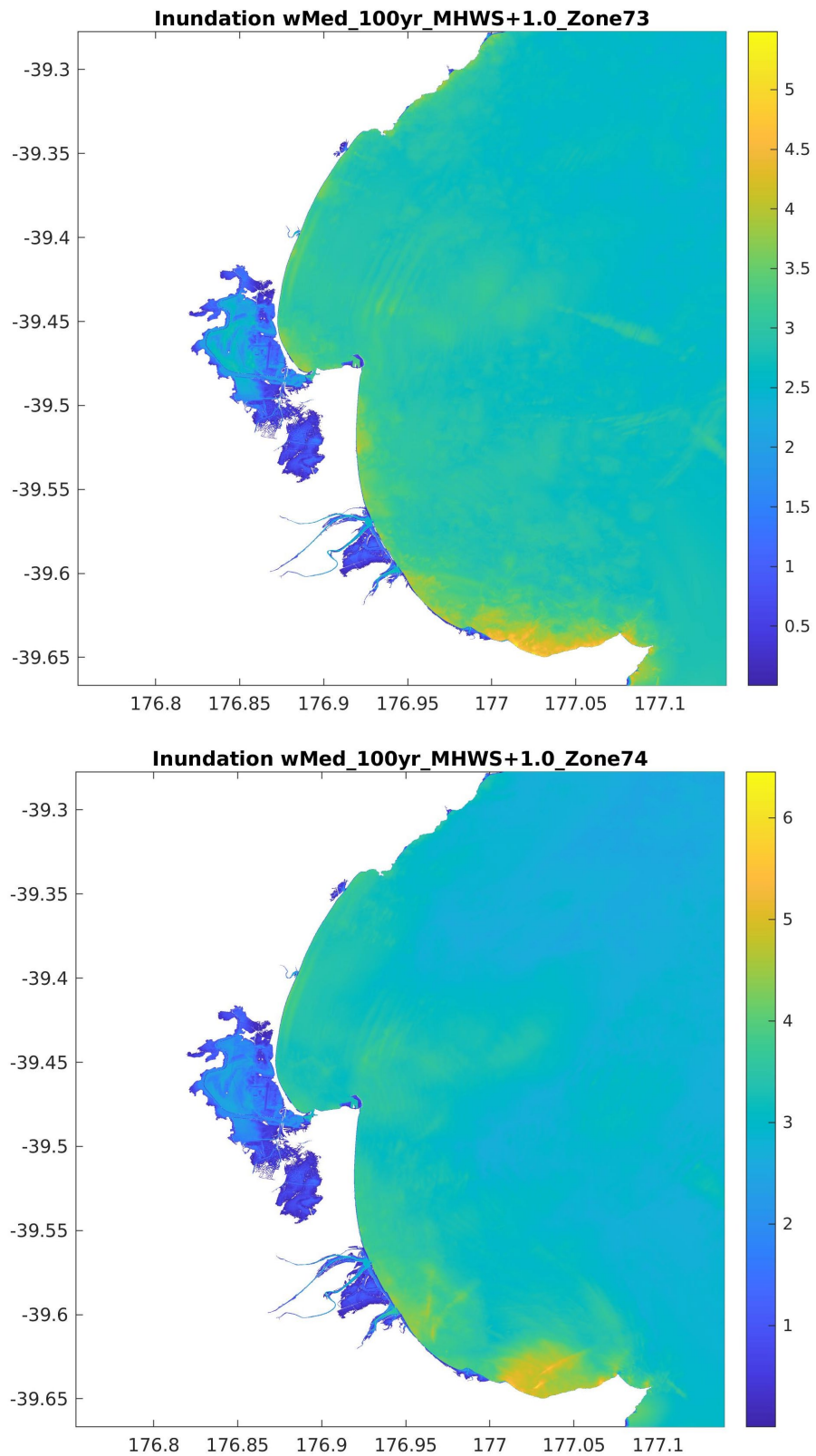


Figure 5.4 Probabilistic tsunami inundation maps for Hawke's Bay showing the median flow depths onshore and offshore tsunami heights with a 1-in-100-years chance of being exceeded per annum at current MHWS plus 1 m of sea-level rise. Onshore values refer to flow depths, while offshore values refer to maximum tsunami heights.

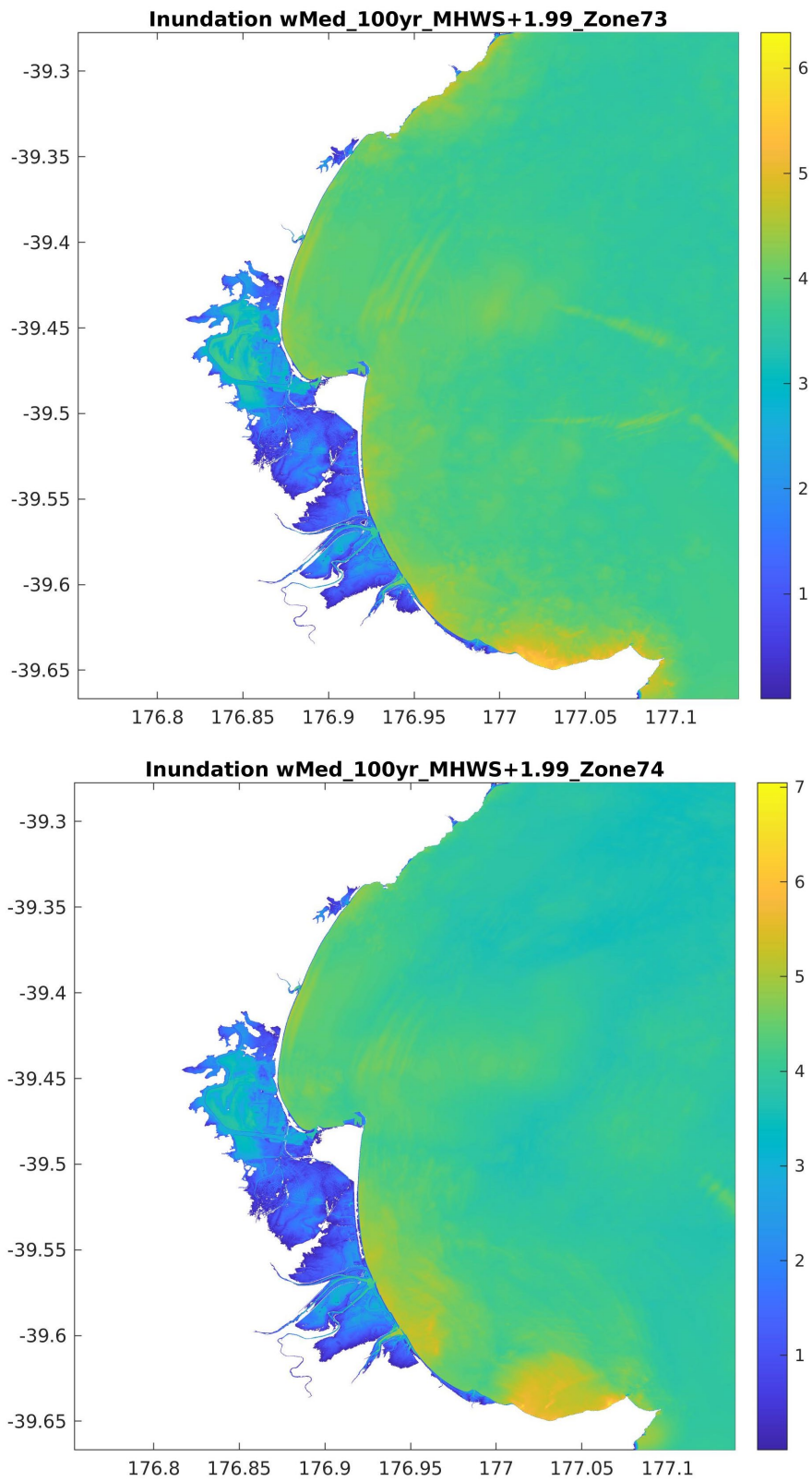


Figure 5.5 Probabilistic tsunami inundation maps for Hawke's Bay showing the median flow depths onshore and offshore tsunami heights with a 1-in-100-years chance of being exceeded per annum at current MHWs plus 1.99 m of sea-level rise. Onshore values refer to flow depths, while offshore values refer to maximum tsunami heights.

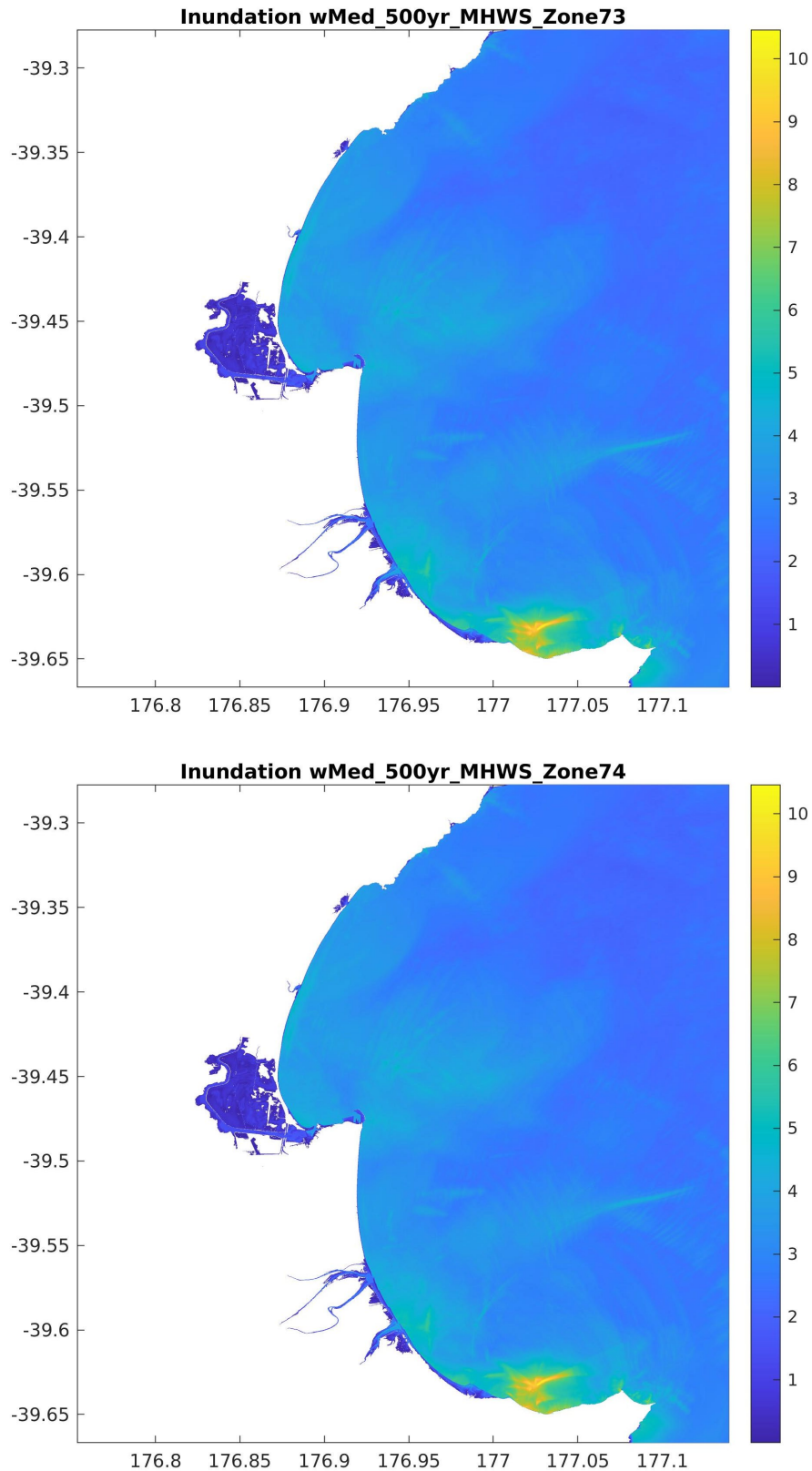


Figure 5.6 Probabilistic tsunami inundation maps for Hawke's Bay showing the median flow depths onshore and offshore tsunami heights with a 1-in-500-years chance of being exceeded per annum at current MHWS. Onshore values refer to flow depths, while offshore values refer to maximum tsunami heights.

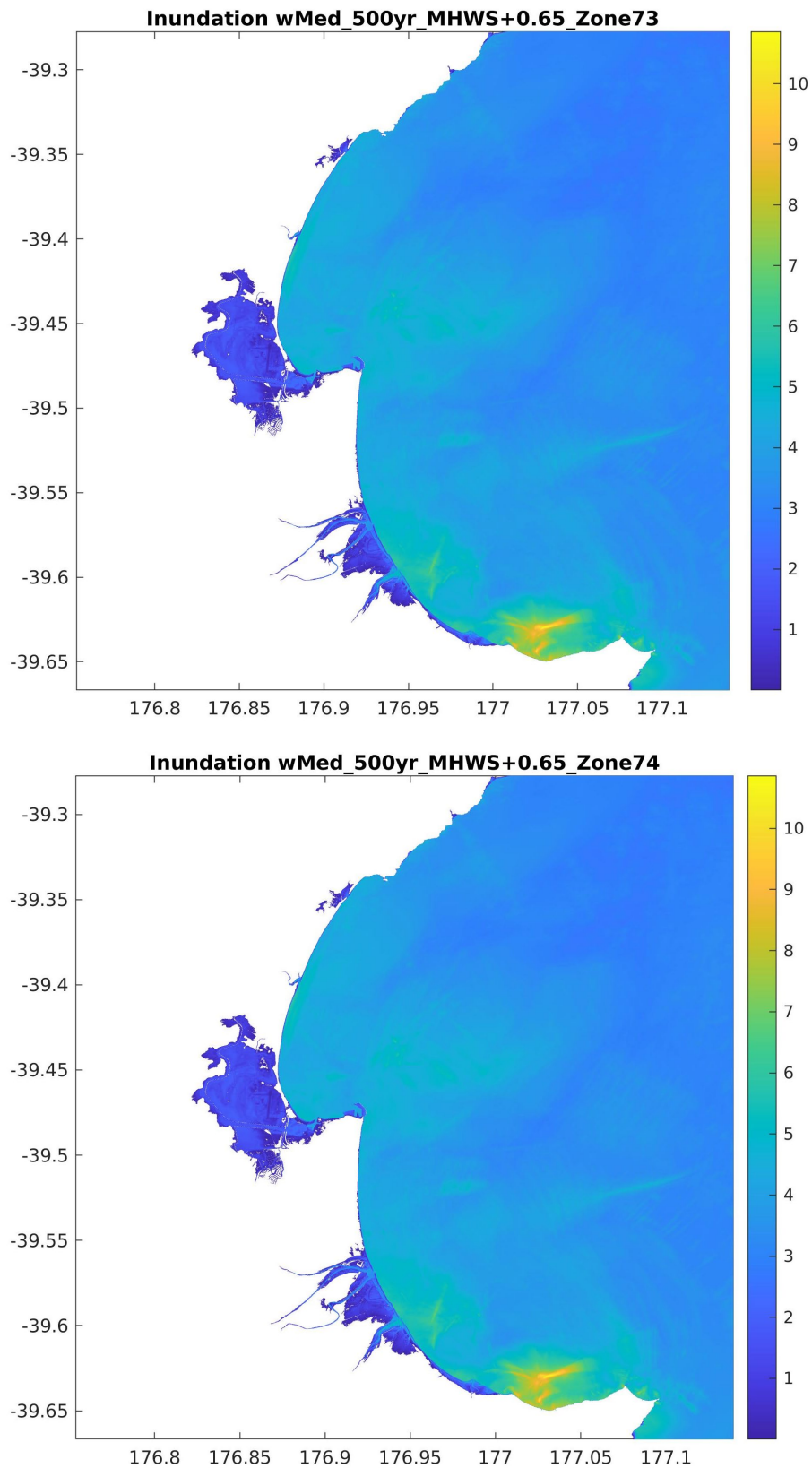


Figure 5.7 Probabilistic tsunami inundation maps for Hawke's Bay showing the median flow depths onshore and offshore tsunami heights with a 1-in-500-years chance of being exceeded per annum at current MHWS plus 0.65 m of sea-level rise. Onshore values refer to flow depths, while offshore values refer to maximum tsunami heights.

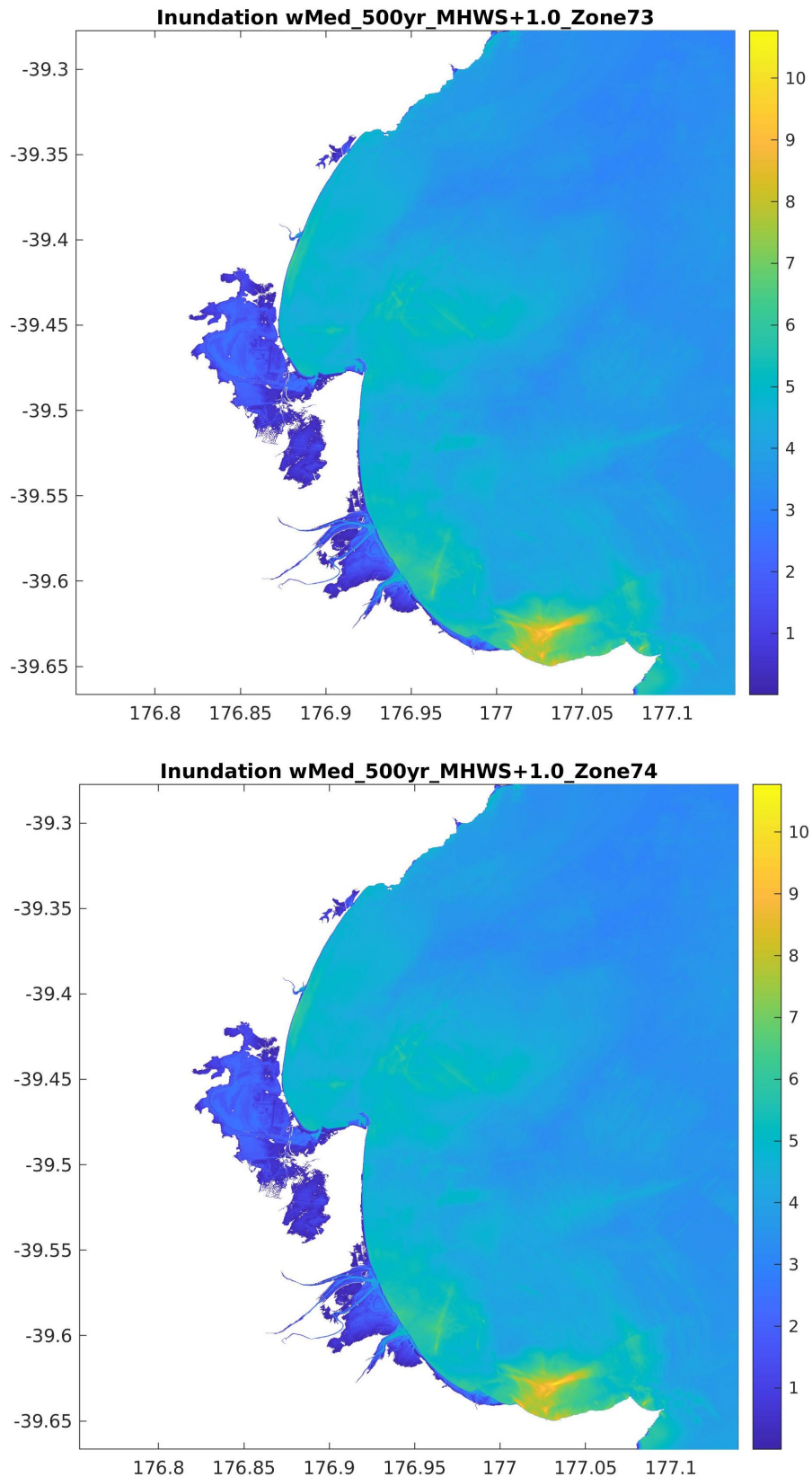


Figure 5.8 Probabilistic tsunami inundation maps for Hawke's Bay showing the median flow depths onshore and offshore tsunami heights with a 1-in-500-years chance of being exceeded per annum at current MHWS plus 1 m of sea-level rise. Onshore values refer to flow depths, while offshore values refer to maximum tsunami heights.

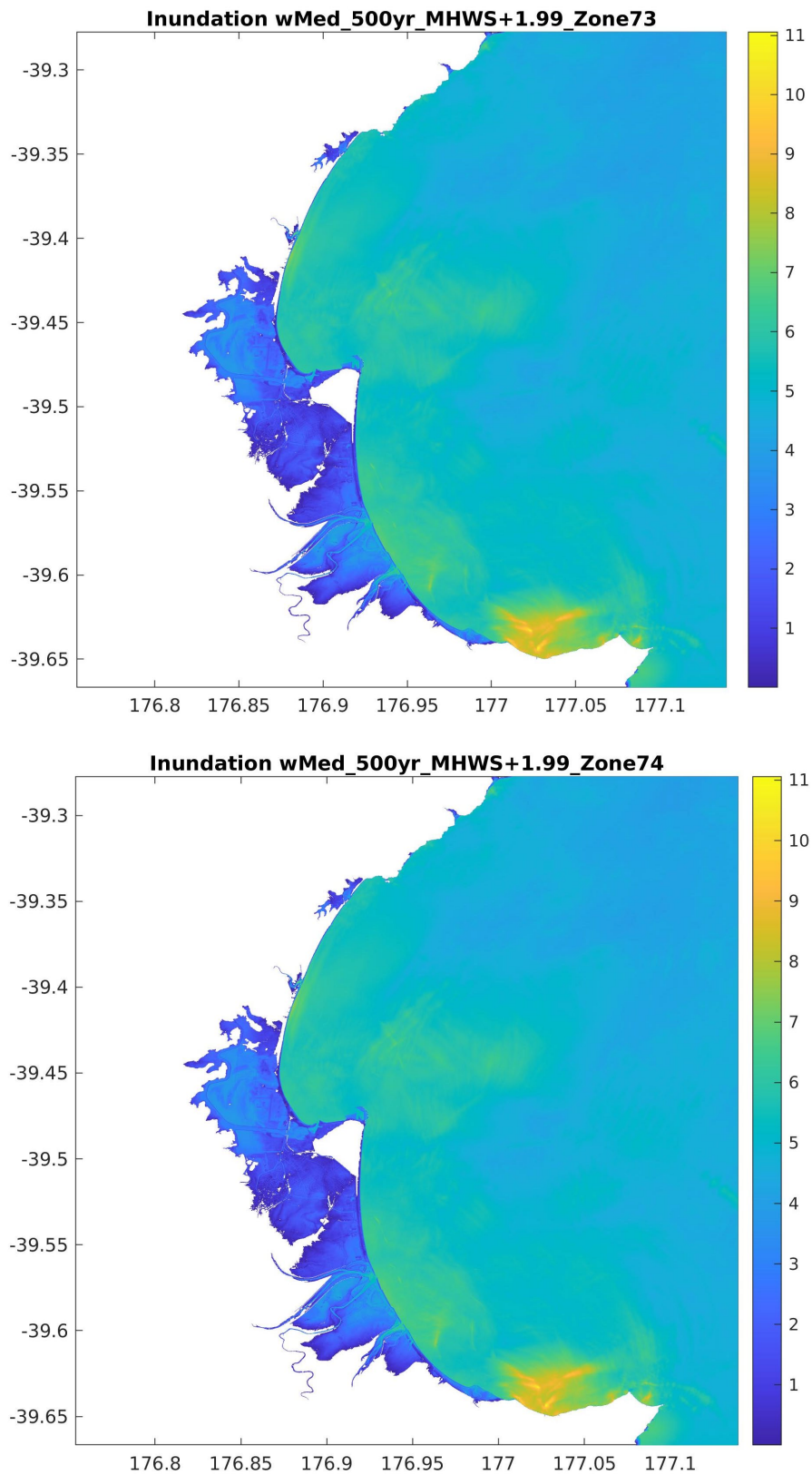


Figure 5.9 Probabilistic tsunami inundation maps for Hawke's Bay showing the median flow depths onshore and offshore tsunami heights with a 1-in-500-years chance of being exceeded per annum at current MHWS plus 1.99 m of sea-level rise. Onshore values refer to flow depths, while offshore values refer to maximum tsunami heights.

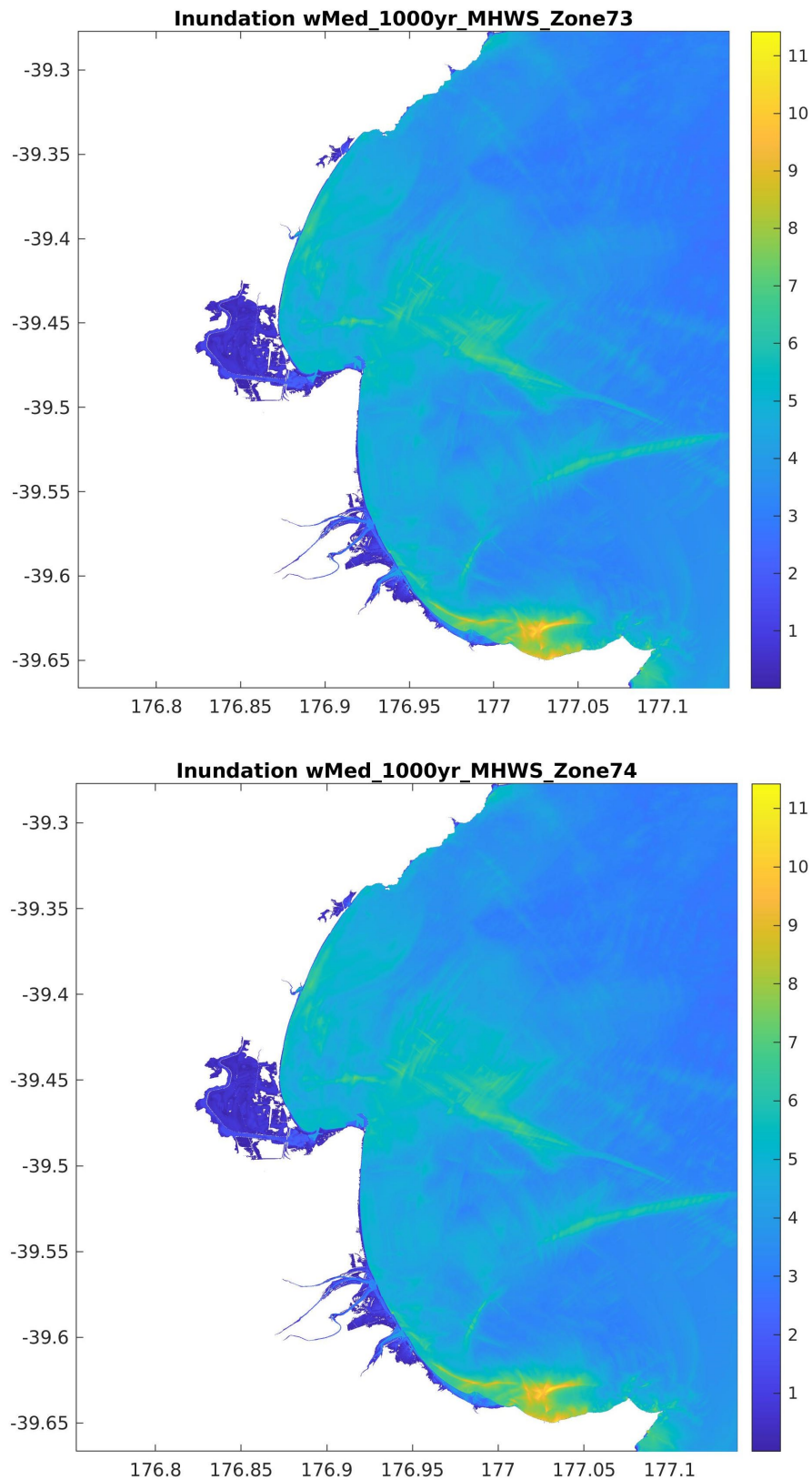


Figure 5.10 Probabilistic tsunami inundation maps for Hawke's Bay showing the median flow depths onshore and offshore tsunami heights with a 1-in-1000-years chance of being exceeded per annum at current MHWS. Onshore values refer to flow depths, while offshore values refer to maximum tsunami heights.

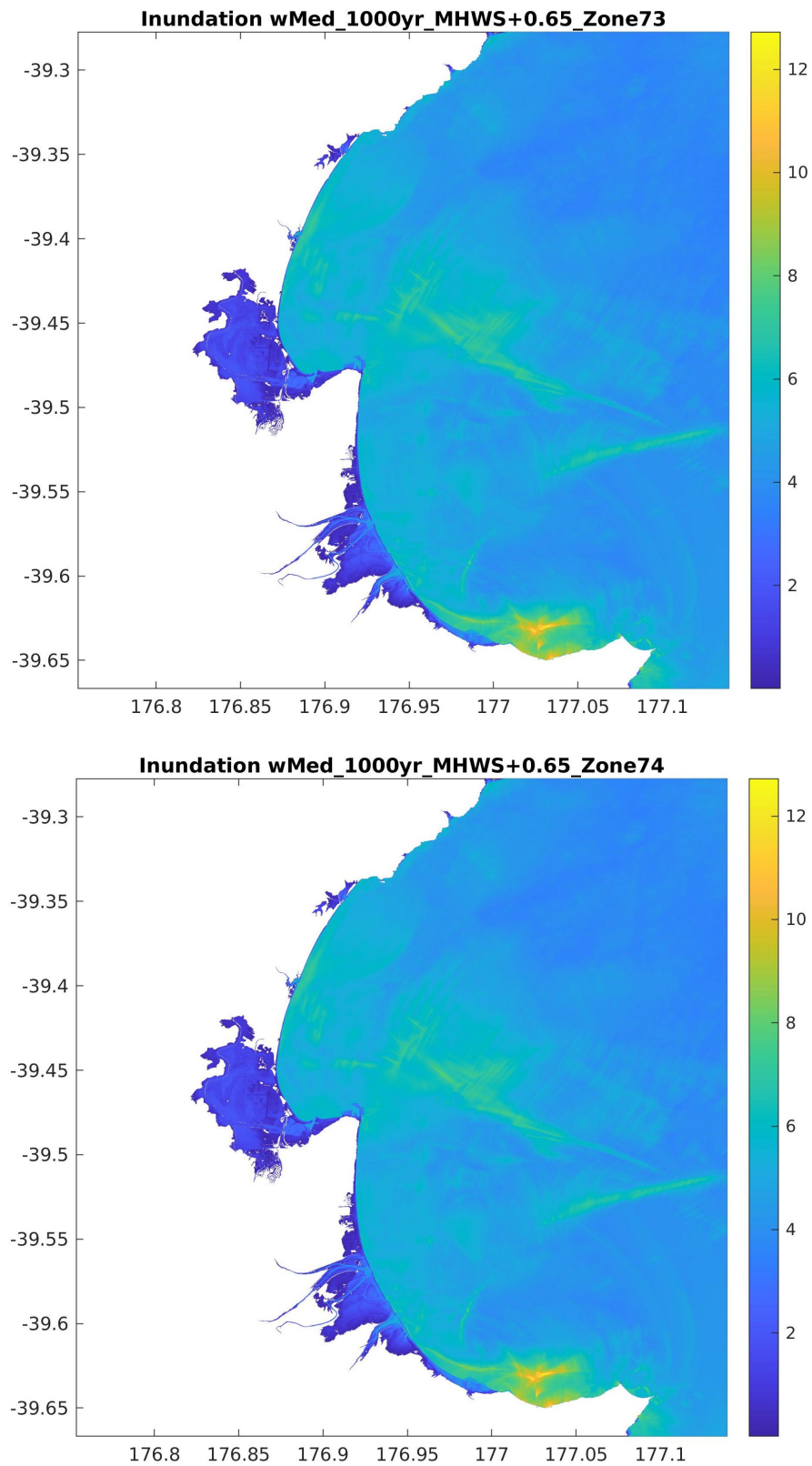


Figure 5.11 Probabilistic tsunami inundation maps for Hawke's Bay showing the median flow depths onshore and offshore tsunami heights with a 1-in-1000-years chance of being exceeded per annum at current MHWS of sea-level rise plus 0.65 m. Onshore values refer to flow depths, while offshore values refer to maximum tsunami heights.

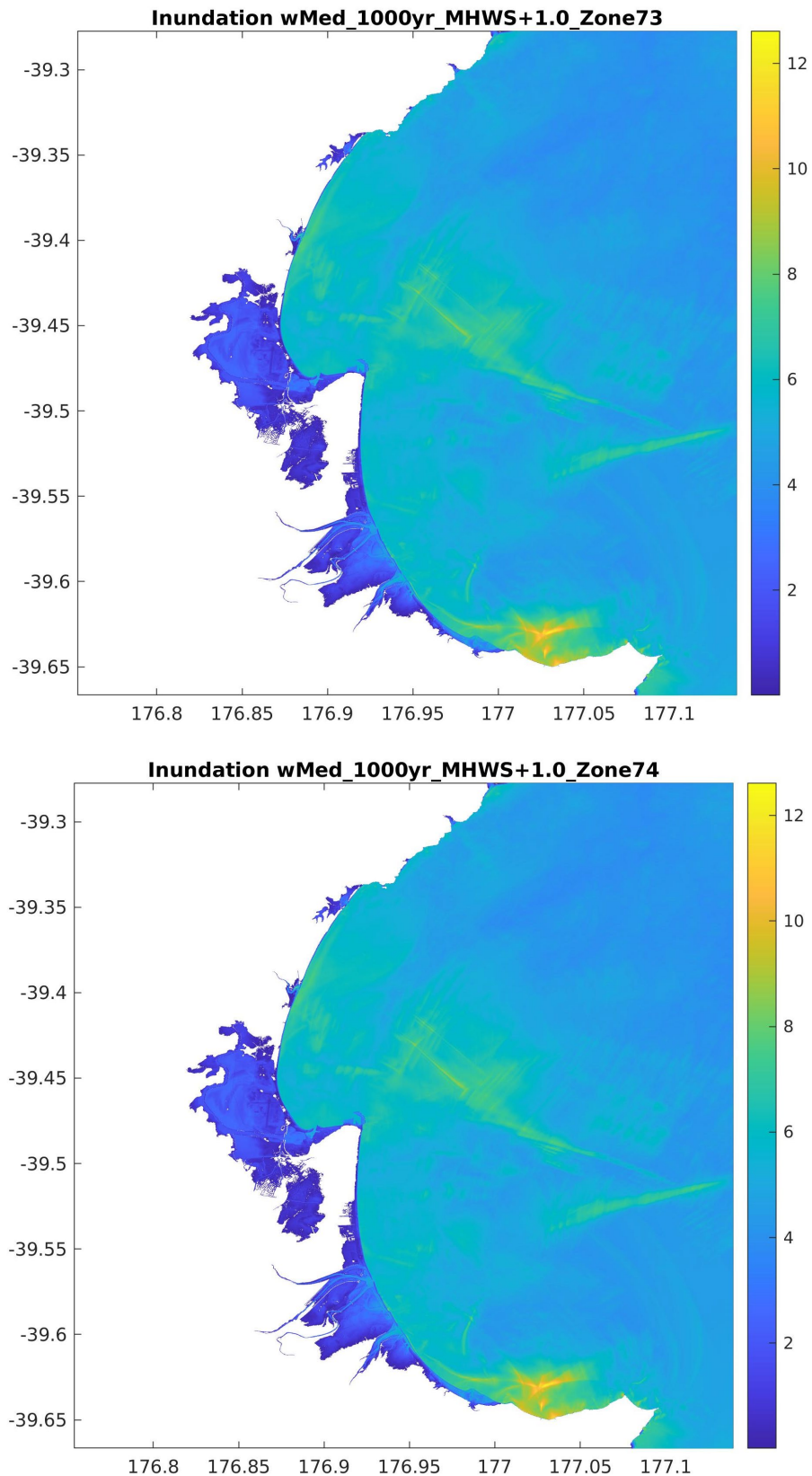


Figure 5.12 Probabilistic tsunami inundation maps for Hawke's Bay showing the median flow depths onshore and offshore tsunami heights with a 1-in-1000-years chance of being exceeded per annum at current MHWS plus 1 m of sea-level rise. Onshore values refer to flow depths, while offshore values refer to maximum tsunami heights.

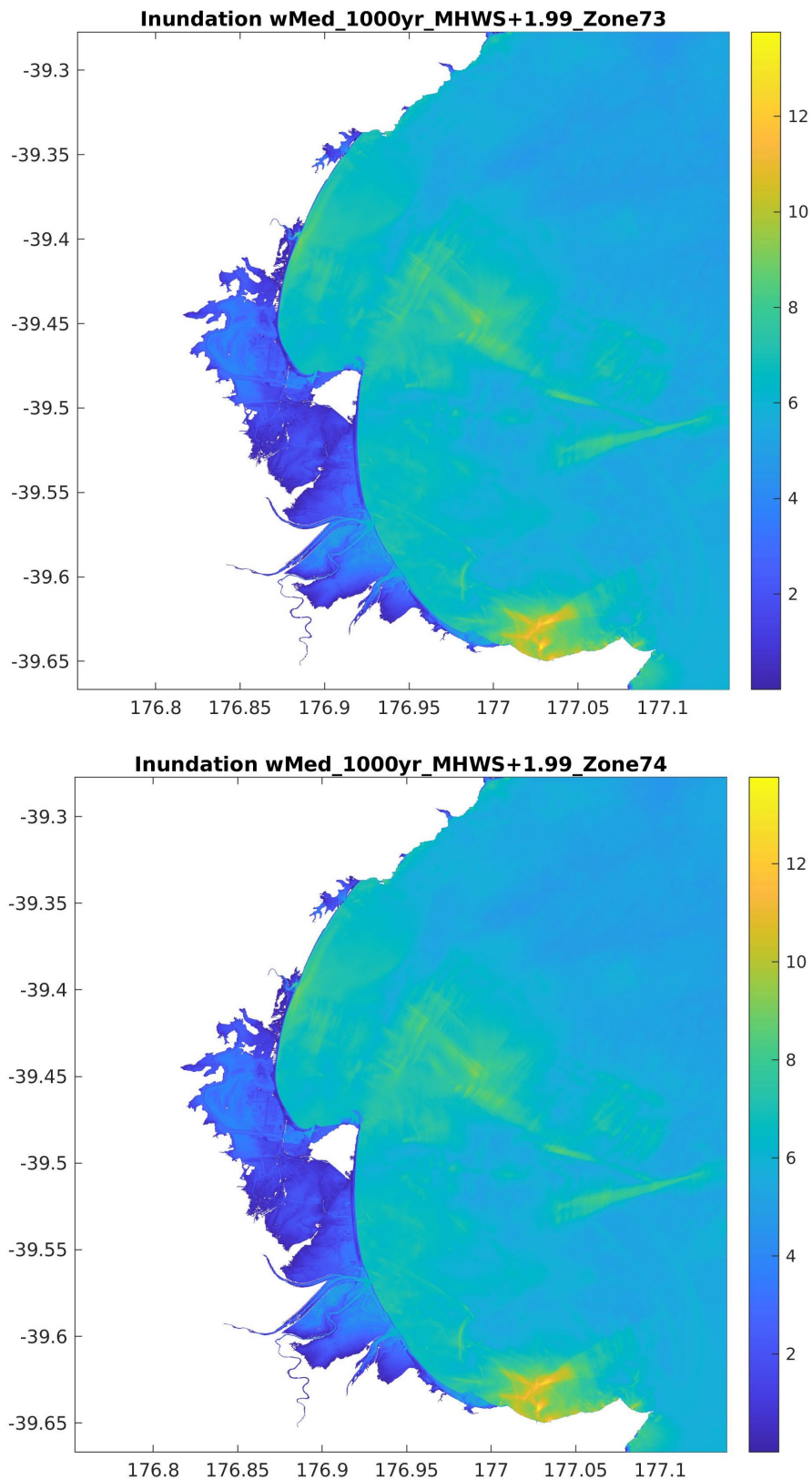


Figure 5.13 Probabilistic tsunami inundation maps for Hawke's Bay showing the median flow depths onshore and offshore tsunami heights with a 1-in-1000-years chance of being exceeded per annum at current MHWS plus 1.99 m of sea-level rise. Onshore values refer to flow depths, while offshore values refer to maximum tsunami heights.

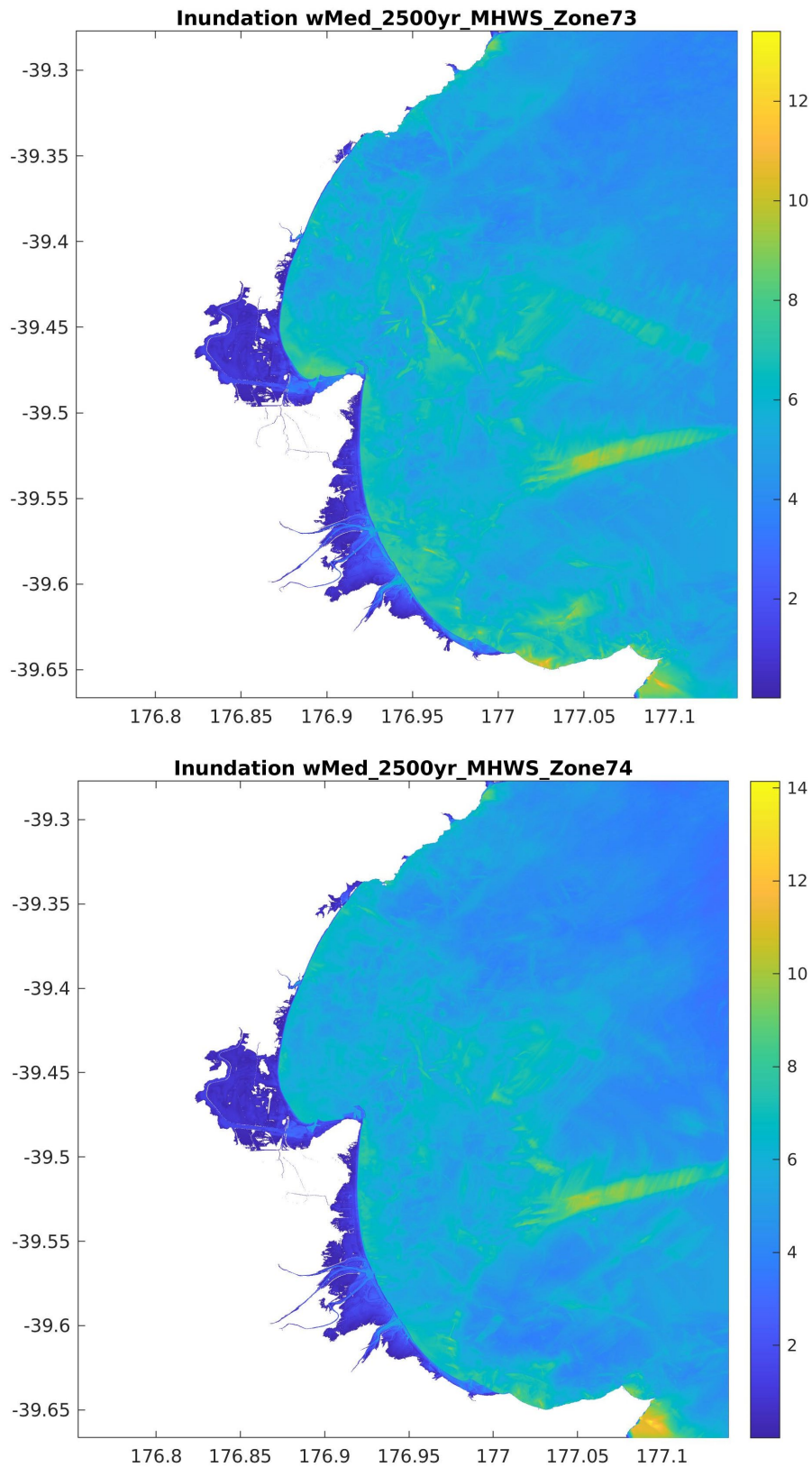


Figure 5.14 Probabilistic tsunami inundation maps for Hawke's Bay showing the 84th percentile flow depths onshore and offshore tsunami heights with a 1-in-2500-years chance of being exceeded per annum at current MHWS. Onshore values refer to flow depths, while offshore values refer to maximum tsunami heights. This is the 'maximum considered tsunami' hazard map for the current sea level.

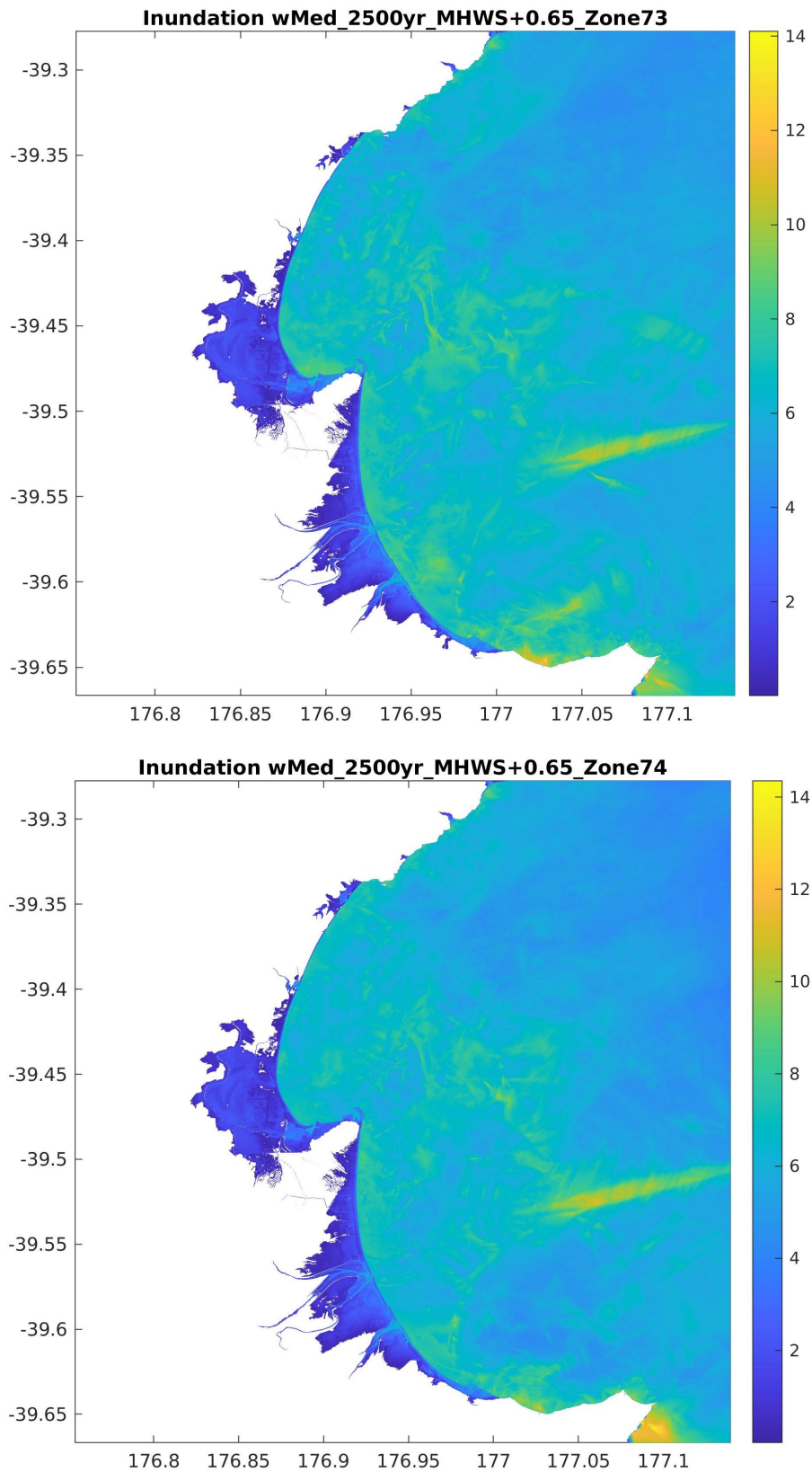


Figure 5.15 Probabilistic tsunami inundation maps for Hawke's Bay showing the 84th percentile flow depths onshore and offshore tsunami heights with a 1-in-2500-years chance of being exceeded per annum at current MHWS plus 0.65 m. Onshore values refer to flow depths, while offshore values refer to maximum tsunami heights. This is the 'maximum considered tsunami' hazard map for this sea-level rise value.

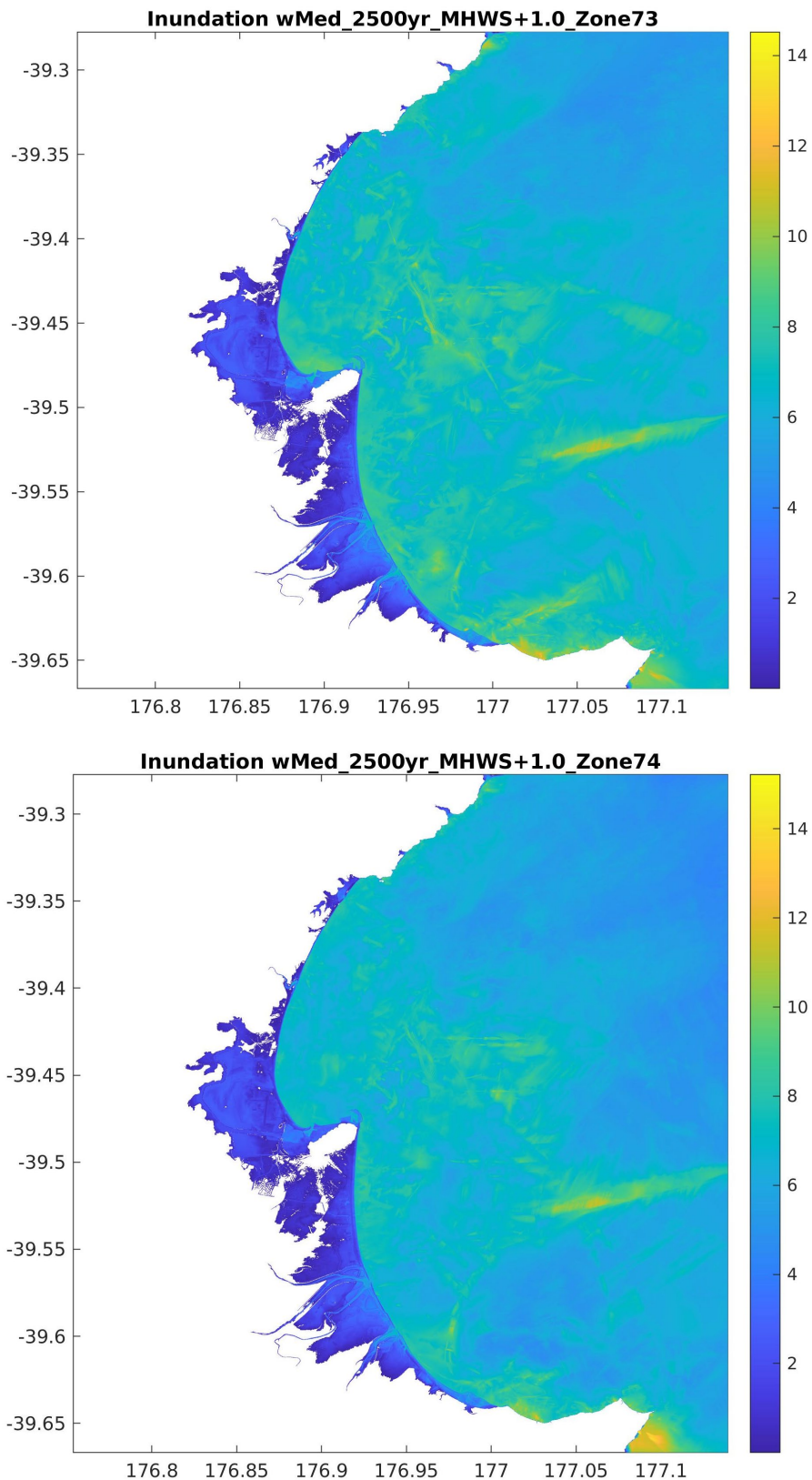


Figure 5.16 Probabilistic tsunami inundation maps for Hawke's Bay showing the 84th percentile flow depths onshore and offshore tsunami heights with a 1-in-2500-years chance of being exceeded per annum at current MHWS plus 1 m. Onshore values refer to flow depths, while offshore values refer to maximum tsunami heights. This is the 'maximum considered tsunami' hazard map for this sea-level rise value.

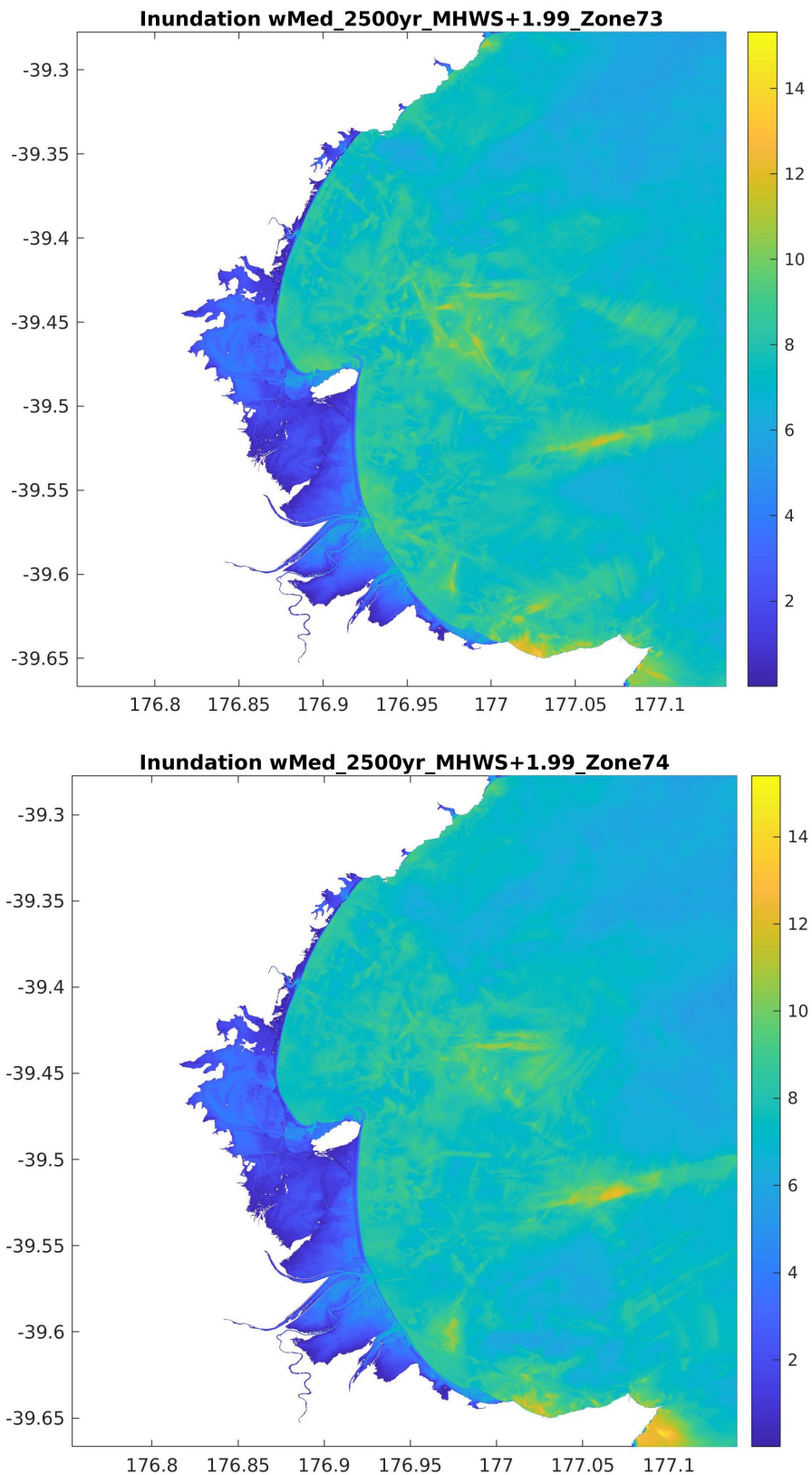


Figure 5.17 Probabilistic tsunami inundation maps for Hawke's Bay showing the 84th percentile flow depths onshore and offshore tsunami heights with a 1-in-2500-years chance of being exceeded per annum at current MHWS plus 1.99 m. Onshore values refer to flow depths, while offshore values refer to maximum tsunami heights. This is the 'maximum considered tsunami' hazard map for this sea-level rise value.

6.0 DISCUSSION

Results presented in Section 5 focused on a set of scenarios that have been directly extracted with the deaggregation methodology considering the return periods asked by HBRC. They do not represent all the scenarios that could exist.

The simulations carry several unknowns that could lead to over- or under-estimation of the actual amount of inundation observed for each scenario and thus in the combined hazard maps. These include uncertainties in modelled digital elevation and bathymetric models, especially in shallow water depths, and surface roughness, as well as variability of the modelled geometry of the rupture surface of the earthquake, non-uniform slip distribution, the sequence in which slip is triggered on that surface and the rake angle specific to individual slip patches. The effects produced by these uncertainties have not been explicitly included in this study for reasons of practicality, although an allowance for some of these effects has been incorporated into the NTHM deaggregation using the idea of an 'effective magnitude' (Power 2013; Power et al. 2022). As a result, while these uncertainties do still exist, we do not believe that they are large enough in magnitude to significantly invalidate the results in Section 5.

This study uses outputs from the NTHM2021 revision, and the uncertainties and limitations of the NTHM (see Power et al. 2022) are applicable to this study. The reader should also note that changes in DEM creation, such as more detailed representation of waterfront and stopbanks, etc., as well as changes in the location of the DEM boundaries, can cause differences in the results presented in this study when compared to the previous studies. Note also that the models run including a sea-level rise component use exactly the same elevation model and land-use model as those run at the current value of MHWS.

Finally, improvements in the models themselves or any of the other inputs, such as the NTHM, could result in changes in the final maps over time. However, GNS Science believes that the models presented here represent the best available maps based on the current science and that are achievable within the resource and time limitations of a project such as this. Thus, they should be suitable to help inform land-use planners and decision makers on how to improve their resilience to tsunami.

This project is related to the three-year EQC-funded research project 'Tsunami impact and Loss Modelling in Hawke's Bay' and to research in the 'Resilience to Natures Challenges 2' (RNC2) Earthquake and Tsunami theme that the EQC project draws upon. The EQC project is primarily focused on loss and risk modelling, mainly using scenarios and hazard maps generated by the RNC2 research. One key difference with this project is the choice of sources and the way in which they are modelled. In the EQC/RNC2 projects, the RSQsim earthquake simulator (Shaw et al. 2022) is used to generate synthetic catalogues of scenarios, likely to include several earthquake scenarios for each fault, rather than selecting a single scenario for a given fault at a specific return period using the deaggregation in the NTHM2021. As the source scenarios are different, it will be highly informative to compare the results of the two studies once the EQC project is complete.

The RSQsim synthetic catalogues currently only include sources that are local to New Zealand, so we should anticipate different and generally smaller inundation extents at short return periods, such as 100 years, in the EQC/RNC2 project, as the NTHM shows a significant contribution to the tsunami hazard from distant sources at shorter return periods. The EQC/RNC2 projects will also be using less-refined tsunami inundation grids than here in order to compensate for the need to run much larger numbers of scenarios in those projects.

The EQC project is focused on the loss and risk modelling methodology, comparing the losses when these are calculated in different ways, and should be informative with regard to the suitability of using hazard maps for loss modelling, as opposed to calculating losses for individual scenarios. With permission from HBRC, the EQC project could also estimate losses for the hazard maps generated in the current project and then compared against losses from the RSQsim-generated scenarios and hazard maps.

Comparisons with the EQC/RNC2 studies will be particularly informative if the NTHM is extended to include inundation at a national scale at a later date. One option for a future NTHM with inundation included is to continue using the 'effective' magnitude to capture the effects of non-uniform slip as in NTHM2021. One uncertainty with this approach is the level at which the magnitude should be increased to account for non-uniform slip, particularly for local sources. The results of this study when compared to those from the EQC and RNC2 studies could be used to help reduce that uncertainty. Another option would be to use the RSQsim catalogue for the NTHM extended to inundation instead of the current method used in NTHM2021. The comparison between the results of this study and the EQC/RNC2 studies will be informative for that option as well. This future work should allow the results of this study to help improve tsunami inundation hazard and risk assessment for the whole country as well as just for the communities in Hawke's Bay.

7.0 ACKNOWLEDGEMENTS

We would like to thank Finn Scheele and Aditya Gusman for reviewing this report.

8.0 REFERENCES

- Arcement GJ Jr, Schneider VR. 1984. Guide for selecting Manning's roughness coefficients for natural channels and flood plains. McLean (VA): US Department of Transportation, Federal Highway Administration. Report FHWA-TS-84-204; [accessed 2021 Sep]. <https://www.fhwa.dot.gov/BRIDGE/wsp2339.pdf>
- Arun PV. 2013. A comparative analysis of different DEM interpolation methods. *The Egyptian Journal of Remote Sensing and Space Science*. 16(2):133–139. doi:10.1016/j.ejrs.2013.09.001.
- Beavan J, Wang X, Holden C, Wilson K, Power W, Prasetya G, Bevis M, Kautoke R. 2010. Near-simultaneous great earthquakes at Tongan megathrust and outer rise in September 2009. *Nature*. 466(7309):959–963. doi:10.1038/nature09292.
- Bricker JD, Gibson S, Takagi H, Imamura F. 2015. On the need for larger Manning's roughness coefficients in depth-integrated tsunami inundation models. *Coastal Engineering Journal*. 57(2):1550005-1–13. doi:10.1142/S0578563415500059.
- Burbidge DR, Gusman AR, Power WL, Wang X. 2021a. Hutt City probabilistic tsunami hazard maps. Lower Hutt (NZ): GNS Science. 26 p. Consultancy Report 2021/115. Prepared for Hutt City Council.
- Burbidge DR, Gusman AR, Power WL, Wang X, Lukovic B. 2021b. Wellington City probabilistic tsunami hazard maps. Lower Hutt (NZ): GNS Science. 24 p. Consultancy Report 2021/91. Prepared for Wellington City Council.
- Fraser S. 2014. Informing the development of tsunami vertical evacuation strategies in New Zealand [PhD thesis]. Wellington (NZ): Massey University. 309 p.
- Fraser SA, Power WL, Wang X, Wallace LM, Mueller C, Johnston DM. 2014. Tsunami inundation in Napier, New Zealand, due to local earthquake sources. *Natural Hazards*. 70(1):415–445. doi:10.1007/s11069-013-0820-x.
- Fujima K. 2001. Long wave propagation on large roughness. In: *Proceedings of the International Tsunami Symposium 2001 (ITS 2001)*; 2001 Aug 7–10; Seattle, Washington. Seattle (WA): NOAA Pacific Marine Environmental Laboratory. p. 891–895.
- Gayer G, Leschka S, Nöhren I, Larsen O, Günther H. 2010. Tsunami inundation modelling based on detailed roughness maps of densely populated areas. *Natural Hazards Earth System Sciences*. 10(8):1679–1687. doi:10.5194/nhess-10-1679-2010.
- Gusman AR, Power WL, Mueller C. 2019a. Tsunami modelling for Porirua City: the methodology to inform land use planning response. Lower Hutt (NZ): GNS Science. 51 p. (GNS Science report; 2019/80).
- Gusman AR, Wang X, Burbidge DR, Lukovic B, Roger JH, Power WL. 2020. Tsunami evacuation zones for West Coast Regional Council. Lower Hutt (NZ): GNS Science. 75 p. Consultancy Report 2020/82. Prepared for West Coast Regional Council.
- Gusman AR, Wang X, Power WL, Lukovic B, Mueller C, Burbidge DR. 2019b. Tsunami threat level database update. Lower Hutt (NZ): GNS Science. 110 p. (GNS Science report; 2019/67).

- Ikechukwu MN, Ebinne E, Idorenyin U, Raphael NI. 2017. Accuracy assessment and comparative analysis of IDW, spline and kriging in spatial interpolation of landform (topography): an experimental study. *Journal of Geographic Information System*. 9:354–371. doi:10.4236/jgis.2017.93022.
- Imamura F, Yalciner AC, Ozyurt G. 2006. Tsunami modelling manual (TUNAMI model); [updated 2006 Apr; accessed 2022 Jun]. https://www.tsunami.irides.tohoku.ac.jp/media/files/_u/project/manual-ver-3_1.pdf
- Kaiser G, Scheele L, Kortenhaus A, Løvholt F, Römer H, Leschka S. 2011. The influence of land cover roughness on the results of high resolution tsunami inundation modeling. *Natural Hazards Earth System Sciences*. 11(9):2521–2540. doi:10.5194/nhess-11-2521-2011.
- Kennedy AB, Chen Q, Kirby JT, Dalrymple RA. 2000. Boussinesq modeling of wave transformation, breaking, and runup. Part1: 1D. *Journal of Waterway, Port, Coastal, and Ocean Engineering*. 126(1):39–47. doi:10.1061/(ASCE)0733-950X(2000)126:1(39).
- Li L, Switzer AD, Wang Y, Chan C-H, Qiu Q, Weiss R. 2018. A modest 0.5-m rise in sea level will double the tsunami hazard in Macau. *Science Advances*. 4(8):eaat1180. doi:10.1126/sciadv.aat1180.
- Liu PLF, Woo SB, Cho YS. 1998. Computer programs for tsunami propagation and inundation. Ithaca (NY): Cornell University. Technical Report.
- Liu Y, Wang X, Wu Z, He Z, Yang Q. 2018. Simulation of landslide-induced surges and analysis of impact on dam based on stability evaluation of reservoir bank slope. *Landslides*. 15(10):2031–2045. doi:10.1007/s10346-018-1001-5.
- Lynett PJ. 2002. A multi-layer approach to modeling generation, propagation, and interaction of water waves [PhD thesis]. Ithaca (NY): Cornell University. 201 leaves.
- Manning R. 1891. On the flow of water in open channels and pipes. *Transactions of the Institution of Civil Engineers of Ireland*. 20:161–207.
- [MCDEM] Ministry of Civil Defence & Emergency Management. 2016. Tsunami evacuation zones: Director's guideline for Civil Defence Emergency Management Groups [DGL 08/16]. Wellington (NZ): Ministry of Civil Defence & Emergency Management; [accessed 2020 Nov]. <http://www.civildefence.govt.nz/assets/Uploads/publications/dgl-08-16-Tsunami-Evacuation-Zones.pdf>
- Mountjoy JJ, Wang X, Woelz S, Fitzsimons S, Howarth JD, Orpin AR, Power WL. 2019. Tsunami hazard from lacustrine mass wasting in Lake Tekapo, New Zealand. In: Lintern DG, Mosher DC, Moscardelli LG, Bobrowsky PT, Campbell C, Chaytor JD, Clague JJ, Georgiopoulou A, Lajeunesse P, Normandeau A et al., editors. *Subaqueous mass movements and their consequences: assessing geohazards, environmental implications and economic significance of subaqueous landslides*. London (GB): Geological Society of London. p. 413–426. (Geological Society special publication; 477).
- Mueller C, Power W, Fraser S, Wang X. 2015a. Effects of rupture complexity on local tsunami inundation: implications for probabilistic tsunami hazard assessment by example. *Journal of Geophysical Research: Solid Earth*. 120(1):488–502. doi:10.1002/2014JB011301.
- Mueller C, Power WL, Wang X. 2015b. Hydrodynamic inundation modelling and delineation of tsunami evacuation zones for Wellington Harbour. Lower Hutt (NZ): GNS Science. 30 p. Consultancy Report 2015/176. Prepared for Wellington Region Emergency Management Office; Greater Wellington Regional Office.

- Mueller C, Wang X, Lukovic B. 2020. Multiple scenario tsunami modelling for the Selwyn coastline, Kaitorete Barrier and Akaroa Harbour. Lower Hutt (NZ): GNS Science. 55 p. Consultancy Report 2020/47. Prepared for Environment Canterbury.
- Mueller C, Wang X, Power WL, Lukovic B. 2019. Multiple scenario tsunami modelling for Canterbury. Lower Hutt (NZ): GNS Science. 63 p. Consultancy Report 2018/198. Prepared for Environment Canterbury.
- Okada Y. 1985. Surface deformation due to shear and tensile faults in a half-space. *Bulletin of the Seismological Society of America*. 75(4):1135–1154. doi:10.1785/BSSA0750041135.
- Power WL, compiler. 2013. Review of tsunami hazard in New Zealand (2013 update). Lower Hutt (NZ): GNS Science. 222 p. Consultancy Report 2013/131. Prepared for Ministry of Civil Defence & Emergency Management.
- Power WL, Burbidge DR, Gusman AR. 2022. The 2021 update to New Zealand's National Tsunami Hazard Model. Lower Hutt (NZ): GNS Science. 63 p. (GNS Science report; 2022/06).
- Power WL, Gusman AR, Wang X, Lukovic B, Black JA. 2019. Pilot tsunami hazard study for Scott Base in Antarctica. Lower Hutt (NZ): GNS Science. 60 p. Consultancy Report 2019/113. Prepared for Antarctica New Zealand.
- Roger JH, Mueller C, Wang X. 2020. Multiple scenario tsunami modelling for northern Pegasus Bay and northern Banks Peninsula bays. Lower Hutt (NZ): GNS Science. 49 p. Consultancy Report 2020/136. Prepared for Environment Canterbury.
- Stirling M, McVerry G, Gerstenberger M, Litchfield N, Van Dissen R, Berryman K, Barnes P, Wallace L, Villamor P, Langridge R, et al. 2012. National seismic hazard model for New Zealand: 2010 update. *Bulletin of the Seismological Society of America*. 102(4):1514–1542. doi:10.1785/0120110170.
- Wang X. 2008. Numerical modelling of surface and internal waves over shallow and intermediate water [PhD thesis]. Ithaca (NY): Cornell University. 245 p.
- Wang X, Holden C, Power W, Liu Y, Mountjoy J. 2020a. Seiche effects in Lake Tekapo, New Zealand, in an Mw8.2 Alpine Fault earthquake. *Pure and Applied Geophysics*. 177(12):5927–5942. doi:10.1007/s00024-020-02595-w.
- Wang X, Liu PLF. 2006. An analysis of 2004 Sumatra earthquake fault plane mechanisms and Indian Ocean tsunami. *Journal of Hydraulic Research*. 44(2):147–154. doi:10.1080/00221686.2006.9521671.
- Wang X, Liu PLF. 2007. Numerical simulations of the 2004 Indian Ocean tsunamis – coastal effects. *Journal of Earthquake and Tsunami*. 1(3):273–297. doi:10.1142/S179343110700016X.
- Wang X, Lukovic B, Power WL, Mueller C. 2017a. High-resolution inundation modelling with explicit buildings: a case study of Wellington CBD. Lower Hutt (NZ): GNS Science. 27 p. (GNS Science report; 2017/13).
- Wang X, Power WL. 2011. COMCOT: a tsunami generation, propagation and run-up model. Lower Hutt (NZ): GNS Science. 121 p. (GNS Science report; 2011/43).
- Wang X, Power WL, Lukovic B, Mueller C. 2017b. Effect of explicitly representing buildings on tsunami inundation: a pilot study of Wellington CBD. In: *Next generation of low damage and resilient structures: New Zealand Society for Earthquake Engineering Annual Conference; 2017 Apr 27–29; Wellington, New Zealand*. Wellington (NZ): New Zealand Society for Earthquake Engineering. Paper O3C.3.

- Wang X, Power WL, Mueller C, Lukovic B. 2020b. Tsunami modelling for proposed cross-harbour pipeline project. Lower Hutt (NZ): GNS Science. 41 p. Consultancy Report 2020/07. Prepared for Wellington Water Limited.
- Wang X, Prasetya G, Power WL, Lukovic B, Brackley HL, Berryman KR. 2009. Gisborne District Council tsunami inundation study. Lower Hutt (NZ): GNS Science. 117 p. Consultancy Report 2009/233. Prepared for Gisborne District Council.
- Wijetunge JJ, Wang X, Liu PLF. 2008. Indian Ocean tsunami on 26 December 2004: numerical modeling of inundation in three cities on the south coast of Sri Lanka. *Journal of Earthquake and Tsunami*. 2(2):133–155. doi:10.1142/S1793431108000293.



www.gns.cri.nz

Principal Location

1 Fairway Drive, Avalon
Lower Hutt 5010
PO Box 30368
Lower Hutt 5040
New Zealand
T +64-4-570 1444
F +64-4-570 4600

Other Locations

Dunedin Research Centre
764 Cumberland Street
Private Bag 1930
Dunedin 9054
New Zealand
T +64-3-477 4050
F +64-3-477 5232

Wairakei Research Centre
114 Karetoto Road
Private Bag 2000
Taupo 3352
New Zealand
T +64-7-374 8211
F +64-7-374 8199

National Isotope Centre
30 Gracefield Road
PO Box 30368
Lower Hutt 5040
New Zealand
T +64-4-570 1444
F +64-4-570 4657